

Replies to referee #1

The authors would like to thank the reviewers for their thoughtful reviews, and constructive comments and suggestions. Our replies are given directly after the comments (in bold); text that has been added/revised is shown in red font.

General comments:

The authors focus on the contribution of particle-particle interaction to growth and determine a maximum error of the growth rate for the collision controlled scenario. They do not explicitly state that this error represents a maximum overestimation of the growth rate (there are several statements mentioning this “upper limit” of the GR [page 3, line 85; page 7 line 191; p 10, line 312] or “maximum possible error” [abstract]; however, it may be interpreted by the reader as the maximum value of the error). It may also be worth mentioning the possibility of GR underestimation caused by deposition losses, dilution and losses to pre-existing particles.

The effect of pre-existing particles on GR errors is discussed as a representative case for several processes (wall loss, dilution and pre-existing particles). This, according to the authors, is justified by findings on the similarity of those processes with regard to effects on the nucleation as described in a recent study (McMurry & Li, 2017). In the present manuscript it is assumed that particle sinks of any form mainly reduce the monomer concentration. Thus, the main effect is the reduction of nucleated particles and this limits coagulation which, according to the authors reduces the error in the GRs. However, loss of particles to the wall, to preexisting particles or by dilution is not considered by the analysis methods discussed and thus potentially lowers the GR obtained from the respective methods (e.g. in a case with low particle growth where uptake of vapor by the walls is limited while the walls may represent a perfect sink for particles). This results in underestimation of the GR.

In the manuscript errors of the analyzed GRs are discussed with regard to the analysis methods applied which are not suitable to produce size and time dependent GRs. The result of those methods is rather an array giving GR for various particle sizes and different measurement times. Further, the methods have inherent errors as they attribute any change of the PSD to growth. Thus, these methods in general are not suitable to produce realistic GR. However, in some specific cases they are. The present manuscript does not provide the necessary information to distinguish between situations where the methods can safely be applied or not. The reason is the fact that possible underestimation of the GR is not discussed (e.g. low GR in a chamber with considerable wall loss and/or dilution may lead to considerable underestimation of the GR by applying one of the methods used). Thus, I suggest removing statements on situations featuring safe usage of those methods and replacing them by statements indicating where the methods cannot/should not be applied. Maybe the authors should also point out once again the possible alternative methods for data analysis which do not suffer from the errors discussed in this manuscript in the conclusion section.

Replies to general comments:

We find the review very constructive and have improved our paper accordingly. Major changes include

1. We added Sect. 3.4 and Fig. 6 in the revised manuscript to qualitatively show that in the presence of strong particle sinks, true growth rate can be underestimated by measured growth rate. In such nucleation scenarios, the particle size distribution approaches steady state after a certain time with the measured growth rate approaching 0, but the true growth rate remains finite and is thus underestimated by measured growth rate.
2. Since we do not study underestimation of growth quantitatively, we changed ‘maximum possible error’ or similar expressions to ‘maximum overestimation of GR_{true} by GR_m ’ or similar expressions throughout the manuscript.

3. Statements regarding safe usage of using measured growth rate as true growth rates have been removed; instead, we mainly focus on the discussing the simulation results presented in the paper and avoid making overly general statements.

Replies to specific comments:

p.2, line 40 (f): “Coagulation is accounted for with the coagulation integrals in the GDE and is a relatively well understood process that can be described with reasonable confidence in models.” A reference would be helpful

We included Chan and Mozurkewich (2001) and Kürten et al. (2018). In the former reference coagulation rates were measured experimentally and Hamaker constant were obtained by fitting experimental data. The result were then applied in the latter reference to analyze CLOUD data.

p.2, line 41 (f): “Growth involves processes that are not well understood for chemically complex aerosol systems, such as the atmosphere.” Reference or examples plus references would be helpful.

We included Barsanti et al. (2009), Riipinen et al. (2012) and Hodshire et al. (2016) as references.

p.4, line 95 (f): “Our results help to inform estimates of uncertainty for complex aerosol systems, such as the atmosphere, where errors are difficult to quantify.” How is this possible as the present manuscript deals with nucleation of a single molecule species which is formed at a constant rate?

We think our original statement is a bit overreaching. The corresponding text now reads “Our results help to inform estimates of uncertainties for systems with a single nucleating species, or systems that can be modeled in a similar way to a single species system (Kürten et al. ,2018).”

p.6, line 158: “and E_k is the particle the evaporation rate”. Remove the second “the”.

‘The’ has been removed.

p.7, line 190 (ff): “We believe collision-controlled nucleation ($E=0$) in the absence of other particle loss mechanisms such as wall deposition ($W=0$) and scavenging by preexisting particles ($\sqrt{L}=0$) provides an upper limit to errors in GR_m for a constant rate system ($R=\text{constant}$).” The error represents a maximum overestimation of the GR. A “maximum error” would also mean that it is bigger than the maximum underestimation of the GR which may not be true. Thus this statement is too general to me.

Agreed. We reworded the sentence to be “We believe collision-controlled nucleation ($E=0$) in the absence of other particle loss mechanisms such as wall deposition ($W=0$) and scavenging by preexisting particles ($\sqrt{L}=0$) provides an upper limit for overestimation of GR_{true} for a constant rate system ($R=\text{constant}$).”

p.7, line 199: “Most noticeably, particles grow considerably faster at early stages of simulation” Do the particles really grow faster or do they seem to grow faster? What is the reason?

The following sentences were added to explain the faster particle growth at the early stage of simulation: “This occurs because evaporation depletes clusters and correspondingly increases monomer concentration. In the absence of pre-existing particles, monomer concentration accumulates until the supersaturation is high enough for nucleation to take place (see figure 2c). The accumulated monomers then rapidly condense on the nucleated particles, leading to the rapid particle growth shown in figure 2b.”

p.9, line 275: “Note for the range of \sqrt{L} values examined, the presence of preexisting particles alter GR_{true}/GR_m values by no more than 50%.” The GR_{true}/GR_m ratio ranges from roughly 0.35 to about 1.1 which is more than 50% (see Fig. 4b)

The original text “Note for the range of \sqrt{L} values examined, the presence of preexisting particles alter GR_{true}/GR_m values by no more than 50%” is a comment on collision-controlled nucleation ($E=0$). Fig. 4b shows the difference between each curve (corresponding to different \sqrt{L} values) is indeed less than 50%. To avoid confusion, “**for collision controlled nucleation**” is added to the original text.

p.10, line 306 (f): “In practice, this means measured growth rate based on all the four representative sizes can be a reasonable substitute of the true growth rate in a similar nucleation scenario.” As the possibility to underestimate the GR is not discussed, this statement does not hold true. Further, “similar nucleation scenario” is a vague statement. When would an experimental set of data be similar?

This sentence has been deleted and the analysis in the revised manuscript is focused only on the simulation results.

p.10. line 312: “Collision-controlled nucleation without preexisting particles results in an upper limit (up to a factor of 6) to discrepancies between true (GR_{true}) and measured (e.g., $GR_{m,mode}$) growth rates.” It could be mentioned that this statement refers to simulated data (e.g.: Simulation showed that collision-controlled) otherwise it is too general.

Agreed. The sentence in question now reads “**Simulated data shows that collision-controlled nucleation without pre-existing particles leads to an upper limit (up to a factor of 6) of overestimating true growth rates (GR_{true}) by modal growth rates ($GR_{m,mode}$).**”

p.10, line 318 (f): “Both evaporation and preexisting particles bring GR_{true}/GR_m closer to unity by decreasing the number of nucleated particles. In the case of evaporation, GR_{true}/GR_m also increases as a result of elevated monomer concentration.” This statement in general is not true. Evaporation and preexisting particles reduce the ratio GR_{true}/GR_m by reducing the overestimation caused by coagulation. In case the GR is underestimated (i.e. $GR_{true}/GR_m < 1$; caused by e.g. wall losses/dilution combined with weak particle growth) by the analysis methods, the combined effect of evaporation and preexisting particles would even increase the error

The sentence now reads “**Both evaporation and scavenging by preexisting particles can reduce the concentration of particles formed by nucleation. Lower particle concentrations reduce the effect of coagulation on GR_m , so overestimation of GR_{true} by GR_m is lower than is found in the absence of these processes**”. In addition, we added section 3.4 to briefly discuss the situation where strong particle sink processes (i.e., sufficiently large values of M or \sqrt{L}) lead to steady state particle size distributions. In these cases, measurements would not reveal any particle growth after a certain time and GR_m would approach 0.

p.10 line 324 (f): “In this case, GR_m based on all representative sizes can be a good approximation of GR_{true} due to negligible coagulation effects.” This statement, similar to the previous one, is too general as it considers only the possible overestimation of the GR (caused by coagulation). However, if the analysis method does not account for methods different from coagulation (e.g. dilution, wall loss, deposition), there may still be a significant difference between the measured and the “true” GR.

This statement has been deleted since it is too general.

Barsanti, K. C., McMurry, P. H., and Smith, J. N.: The potential contribution of organic salts to new particle growth, *Atmos. Chem. Phys.*, 9, 2949-2957, 10.5194/acp-9-2949-2009, 2009.

Chan, T. W., and Mozurkewich, M.: Measurement of the coagulation rate constant for sulfuric acid particles as a function of particle size using tandem differential mobility analysis, *Journal of Aerosol Science*, 32, 321-339, [https://doi.org/10.1016/S0021-8502\(00\)00081-1](https://doi.org/10.1016/S0021-8502(00)00081-1), 2001.

Hodshire, A. L., Lawler, M. J., Zhao, J., Ortega, J., Jen, C., Yli-Juuti, T., Brewer, J. F., Kodros, J. K., Barsanti, K. C., Hanson, D. R., McMurry, P. H., Smith, J. N., and Pierce, J. R.: Multiple new-particle growth pathways observed at the US DOE Southern Great Plains field site, *Atmos. Chem. Phys.*, 16, 9321-9348, 10.5194/acp-16-9321-2016, 2016.

Kürten, A., Li, C., Bianchi, F., Curtius, J., Dias, A., Donahue, N. M., Duplissy, J., Flagan, R. C., Hakala, J., Jokinen, T., Kirkby, J., Kulmala, M., Laaksonen, A., Lehtipalo, K., Makhmutov, V., Onnela, A., Rissanen, M. P., Simon, M., Sipilä, M., Stozhkov, Y., Tröstl, J., Ye, P., and McMurry, P. H.: New particle formation in the sulfuric acid–dimethylamine–water system: reevaluation of CLOUD chamber measurements and comparison to an aerosol nucleation and growth model, *Atmos. Chem. Phys.*, 18, 845-863, 10.5194/acp-18-845-2018, 2018.

Riipinen, I., Yli-Juuti, T., Pierce, J. R., Petäjä, T., Worsnop, D. R., Kulmala, M., and Donahue, N. M.: The contribution of organics to atmospheric nanoparticle growth, *Nature Geoscience*, 5, 453, 10.1038/ngeo1499, 2012.

Replies to referee #2

The authors would like to thank the reviewers for their thoughtful reviews, and constructive comments and suggestions. Our replies are given directly after the comments (in bold); text that has been added/revised is shown in red font.

General comments:

In this study uncertainties in particle growth rates are investigated using model simulations. More specifically, the authors study how significantly the particle growth rates determined using different methods deviate from the growth rate due to vapor condensation. They show that this difference is largest in the system where the growth is collision-controlled and vapor concentrations are high, in which case the growth due to coagulation becomes significant. In the presence of sink due to pre-existing particles and evaporation, the coagulation growth is less significant and thus also the difference between the measured growth rate and the condensation growth rate is smaller.

The study seems scientifically sound and the presented results are interesting to the scientific community as the growth rate methods discussed in the manuscript are generally used when analyzing particle size distribution data. Therefore, I recommend the manuscript for publication in ACP after the authors have considered the comments listed below and the comments presented by Referee #1.

Replies to specific comments:

P1, L1: This study does not actually discuss the errors in nanoparticle growth rates but the difference between the measured growth rate and the growth rate caused by vapor condensation. These are separate issues because the growth due to collisions of small clusters (coagulation growth) is also real growth. Please modify the manuscript to make this clear (title, abstract, conclusions, and rest of the text).

The reviewer correctly argues that collisions of small clusters can contribute to growth. We showed that the effect of those coagulation processes on particle growth rates (GR) can be significant for collision-controlled nucleation (Fig. 2a) but are much less important when cluster evaporation occurs to a significant extent (Fig. 2b). The reviewer argues that we should include growth due to cluster coagulation in our definition of “true” particle growth rates, GR_{true} . While there is some logic to this argument, we believe there is an even stronger argument to exclude growth due to cluster coagulation in the GR (which we later define as the “true” growth rate GR_{true}) and dd_p/dt terms defined by E1. 1 and 2 in our manuscript. Our argument might be viewed as merely semantic, but we believe it is more fundamental than this.

First, we acknowledge without question that the discovery of Lehtipalo and coworkers (2016), that clusters can contribute significantly to particle growth rates was a very significant discovery. It is important to understand all processes that contribute to growth, and this was the first paper to show explicitly that cluster coagulation is a significant contributor.

However, as the aerosol general dynamic equation has been formulated for several decades, cluster coagulation is explicitly included in the coagulation terms of the GDE and not in growth rate expression. This does not suggest that quantifying the contribution of cluster to growth is easy. Indeed, it is only recently that cluster distributions could be measured with sufficient accuracy to quantify this effect, and it is not done routinely in most studies. However, once these distributions are known, their dynamic behavior is logically included in the coagulation terms of the cluster balance equations. This allows one to account for the contributions of clusters to particle growth, as well as cluster-cluster coagulation for smaller particles, which can also be significant (Kurten 2018).

Because the reviewer refers to cluster coagulation as a growth process, we believe s/he would agree that it is described by the coagulation terms of the GDE. If so, however, it cannot also be included in the growth term of the GDE, which applies to the net rate of particle growth due to molecular uptake (including condensation, evaporation, and other heterogeneous processes). In addition to the mathematical arguments for not including cluster condensation as part of the growth term in the GDE, there are also conceptual arguments. If the cluster distribution is measured with sufficient accuracy to allow the effects of cluster coagulation on GR_m to be quantified, that is a major step towards reconciling GR_m with processes known to contribute towards particle growth. If large discrepancies remain after accounting for condensation, evaporation and cluster coagulation, that would underscore the need to study other types of processes that could also contribute (e.g., heterogeneous chemical reactions on or within particles.) Such heterogeneous processes are not understood, and the extent to which they may contribute to growth needs to be quantified.

Accordingly, we have not revised the manuscript to include cluster coagulation as a process that is included in our expression for “ GR_{true} ”. We have chosen to conform to the original definition of growth by Friedlander, Seinfeld and their colleagues, and to only include molecular uptake for this term while acknowledging and quantifying the extent to which cluster coagulation can also contribute to growth.

P1, L18–20: It may be confusing for the reader to state that in the presence of pre-existing particles coagulation is reduced. You could make this clearer by writing, for example, “by reducing growth due to coagulation”. The difference between coagulation losses of small particles due to pre-existing larger particles and coagulation growth caused by collisions of small clusters should be made clearer also elsewhere in the manuscript.

To be more specific about what coagulation is referred to, the sentence now reads ‘This can lead to decreased discrepancies between measured growth rate and condensational growth rate by reducing coagulation between nucleated particles.’

P2, L25: Instead of “growth”, I would suggest writing here “condensation and evaporation” as all the other processes are also mentioned separately.

“Growth” in this introductory sentence refers to all processes that lead to particle growth by molecular uptake. The subsequent paragraphs explain that these processes include condensation and evaporation, acid-base reactions, accretion, liquid phase chemical reactions, etc. Therefore, growth is not synonymous with condensation and evaporation in this context. We later explain that in this paper, the only growth processes that we include in this analysis are condensation and evaporation. However, it would be misleading to imply in the introduction that those are the only possible growth processes in general.

P2, L28: Removal of molecular species from a cluster cannot really be called “growth”. Also, when discussing particle growth, it would be good to specify which size range is meant.

We give the definition of ‘growth’ here as net particle size change to addition or removal of molecular species. The sentence now reads ‘Following established conventions long used in modeling aerosol dynamics (Friedlander, 2000; Gelbard and Seinfeld, 1979, 1980), we define the particle “growth rate” as the net rate of change in diameter of individual particles due to the addition or removal of molecular species. (If evaporation exceeds addition, the growth rate would be negative.)’

The result presented in this paper is germane to particle growth up to around 40 nm. This information is given in the second to last paragraph in the introduction.

P2, L38–39: The difference between coagulation scavenging and the growth due to coagulation should be made clear also here. For example, writing “it is worthwhile to treat growth due to condensation and coagulation separately” would make this more understandable. In addition,

although coagulation scavenging is rather well understood, the contribution of collisions of molecular clusters to the growth is not.

We agree that when interpreting experimental data, it would only be possible to account for all coagulation processes if the entire number distribution down to and including clusters of size 2 were accurately measured. However, if such data are available, contributions of coagulation to GR_m , can be accurately assessed. This is true for both coagulation scavenging and coagulation of the freshly nucleated particles. Because we understand our simulated data perfectly, we know those number distributions and can accurately calculate the effects of all coagulation interactions on GR_m . We clearly define growth as due to only to the net rate of molecular uptake (excluding all coagulation processes), thereby distinguishing between GR_{true} and GR_m . We have added the following sentence to clarify this:

'The extent to which the coagulation of freshly nucleated molecular clusters contributes to measured growth rates can be accurately determined only if the entire number distribution down to clusters of size 2 is accurately measured. In the absence of such data, the contributions of cluster coagulation to growth could erroneously be attributed to vapor uptake.'

P2, L45: Please add references here for previous observations on GR.

We included Stolzenburg et al. (2005), Wang et al. (2013), Riccobono et al.(2012) and Tröstl et al.(2016) as references.

P3, L56: GR is usually determined by linear fitting to diameter vs time data, instead of looking only at the difference between two sizes.

Agreed. The sentence now reads 'The growth rate is obtained by first fitting a linear function of particle diameter (corresponding to the size bins) vs. time, and then calculating the slope of the fitted function'.

P3, L58: This method has also been applied in several studies for sub-3 nm particle size distribution data not measured by CPC batteries.

Agreed. The sentence now reads 'This approach has been used to analyze data from condensation particle counter (CPC) batteries (Riccobono, 2014), particle size magnifier (PSM) (Lehtipalo 2014), etc.'

P3, L71: Please add a reference when discussing previous work. Also, this paragraph could fit better in the beginning of the introduction as it provides the general motivation of this work.

We have included the following references: Kontkanen et al.(2016), Riipinen et al.(2012), Hodshire et al.(2016), Smith et al. (2010), Smith et al. (2008) and Tröstl et al.(2016).

We agree that this paragraph fits better at the beginning of the introduction. Therefore, we combined this paragraph with the first paragraph of the introduction.

P3, L79: You should make it clear already here that you define GR_{true} so that it is GR only due to vapor condensation.

Please refer to the response to the first specific comment.

P3, L82: GR_{true} is defined in a different way by Kontkanen et al. (2016) and therefore using the same name for it is misleading.

To make clear the difference between GR_{true} and the related concepts used by Kontkanen et al. (2016), the line now reads 'For example, Kontkanen (2016) used simulations to show that discrepancies between measured growth rate based on appearance time (AGR) and growth rate based on irreversible vapor condensation (CGR) can be significant. (Note GR_{true} used in this paper differs from CGR in that GR_{true} also incorporates evaporation.)'

P4, L103–116: The description of the model and model simulations could be slightly more detailed. The reader should understand the model without a need to look at the earlier publications.

Since loss to pre-existing particles and dilution are discussed in the manuscript, we added the definition of \sqrt{L} and M in the text (Eq. (3) and Eq. (4) in the revised manuscript). In addition, to better explain the model, we added the following text before introducing Eq.(6): ‘**The solution to the GDE for a constant rate system ($R=\text{constant}$) depends on dimensionless time, cluster size and the dimensionless variables \sqrt{L} , M , E , Ω , etc., but is independent of the rate at which condensing vapor is produced by chemical reaction. That rate is required to transform the computed nondimensional solutions to dimensional results using simple multiplicative expressions given by McMurry and Li (2017):**’.

In order for the reader to thoroughly understand what is discussed in the paper under review, she or he will need to read McMurry and Li (2017).

P4, L119: Although using dimensionless parameters certainly has its benefits, it makes comparison between these results and experimental observations or previous simulations difficult. Therefore, also mentioning the values of corresponding dimensional variables (e.g. number concentration, diameter, GR, loss rate) for some of the key results (either in the text or in the figures) would be beneficial.

This is a good suggestion. To facilitate comparison between dimensionless and dimensional results, we converted selected cases discussed in section 3.3 with assumed monomer production rates. The converted dimensional results are shown in Appendix B and Fig. B1.

P7, L199: The fact that the particle growth rate due to condensation and evaporation is higher when there is evaporation in the system is difficult to understand.

To better explain this we added the following sentence: ‘Most noticeably, particles grow considerably faster at early stages of simulation. This occurs because evaporation depletes clusters and correspondingly increases monomer concentration. In the absence of pre-existing particles, monomer concentration accumulates until the supersaturation is high enough for nucleation to take place (see figure 2c). The accumulated monomers then rapidly condense on the nucleated particles, leading to rapid particle growth shown in Fig. 2b.’

P8, L230: Could you add a short explanation why different representative sizes follow this order?

This is an empirical result specific to the nucleation scenario discussed in this paper. We are not sure if this applies to all nucleation scenarios. As a result, we chose not to speculate as to whether or not this order might be a general result for all growth scenarios.

P8, L238: Instead of referring to Eq. (6), could you explain the reason for higher GR?

Some explanation is added to the end of the sentence. ‘**This is partly due to higher monomer concentrations (see red solid curve in Fig. 2c) and partly due to Eq. (6) that leads to higher true growth rate for smaller particles: the addition of a monomer leads to a bigger absolute as well as fractional diameter growth for small particles.**’

P8, L242: This is now slightly unclear. Do you mean that the growth is first slow and then it accelerates?

Yes, the clusters containing a few monomers grow slowly due to the strong Kelvin effect. And particle growth then accelerates when the nucleation burst takes place. To make the text clearer, the paragraph is partially rewritten as follows: ‘**Figure 3d-3f are counterparts of Fig. 3a-3c, but with evaporation constant E set to 1×10^{-3} . Figure 3d shows that $\tilde{d}_{p,sr50}$ and $\tilde{d}_{p,tot50}$ increase relatively slowly at the start of the simulation (see the amplified figure at the lower right corner of Fig. 3d; for reference, the dimensionless sizes of monomer, dimer and trimer are 1.24, 1.56 and 1.79 respectively). Subsequently, a marked change**

slope of the $\tilde{d}_p = \tilde{d}_p(\tau)$ curve is observed, indicating accelerated particle growth. This reflects that nucleation occurs with a burst of particle formation following a process of monomer and cluster accumulation. The slow growth of the smallest clusters is an indication that the accumulation process is slow due to the strength of the Kelvin effect.'

P8, L245: What do you mean by using quotation marks with ‘slow’?

The quotation mark has been deleted.

P8, L248: Some of the measured GRs are in the beginning of the simulation lower than GR_{true} . This means that if evaporation rate was very high, the difference between GR_m and GR_{true} could possibly be larger than in the collision-limited case which is said to correspond to the case with “the maximum possible error”.

This is also pointed out by the other referee: GR_m can be lower than GR_{true} . We didn't quantify underestimation of GR_{true} by GR_m in our revised manuscript. Therefore, to be more precise, we changed ‘maximum possible error’ to ‘maximum overestimation of GR_{true} ’ wherever this is necessary.

P9, L253: But there seems to be even higher values at sizes lower than [10, 15]?

[10, 15] has been changed to be [5, 11].

P9, L262: How does the coagulation sink depend on particle size in your simulations? When stating the range of \sqrt{L} used in the simulations, it would be useful to mention the corresponding range for the dimensional variable.

The dependence of loss rate to preexisting particles is $\sqrt{L}/k^{1/2}$, where k is the number of monomer in a particle. This information is now given in the revised manuscript after Eq. (3) is introduced.

P9, L274: This result sounds counterintuitive. Would the situation change if higher values of \sqrt{L} were used? Does this situation correspond to the situation in the atmosphere? The collision-limited case probably occurs in the atmosphere in polluted environments where losses due to pre-existing particles are very high.

We varied \sqrt{L} values from 0 to 1 (results are not shown in the manuscript), and the monomer concentration varied by less than 10% for collision controlled simulation, though the number of nucleated particles decreased significantly. Dimensionally, if the monomer production rate is $R = 1 \times 10^6 \text{ cm}^{-3} \text{ s}^{-1}$, the monomer has a volume of $1.62 \times 10^{-22} \text{ cm}^3$ with a density of 1.47 g cm^{-3} and the monomer collision frequency function $\beta_{11 fm}$ is $4.27 \times 10^{-10} \text{ cm}^3 \text{ s}^{-1}$, $\sqrt{L}=1$ corresponds to a Fuchs surface area $A_{Fuchs} = 392 \text{ } \mu\text{m}^2 \text{ cm}^{-3}$. This surface area is on the higher end of those observed in the atmosphere (Kuang et al. ,2010). Therefore, the results presented here are relevant to the atmosphere.

P11, L318–319: This conclusion is unclear as it is stated that GR_{true}/GR_m both becomes closer to unity and increases due to evaporation.

Taking into account the possibility of underestimation GR_{true} by GR_m , this conclusion now reads ‘Both evaporation and scavenging by preexisting particles can reduce the concentration of particles formed by nucleation. Lower particle concentrations reduce the effect of coagulation on GR_m , so overestimation of GR_{true} by GR_m is lower than is found in the absence of these processes’.

Technical comments

P1, L18: Please add “that” after “show.

P6, L179: There is no need to repeat the name of the author twice.

P6, L182: Check the subscript.

P6, L188: Please add an en dash to show the range (also elsewhere).

P7, L215: Remove “of”.

P8, L231: Please add “that” after “indicate”.

P8, L248: Check the subscripts.

P9, L275: Please add “that” after “Note”.

Figure 1: Please also mention what *dp,min* stands for in the figure caption.

The manuscript has been revised according to the referee’s technical comments.

Friedlander, S. K.: Smoke, dust, and haze : fundamentals of aerosol dynamics, 2nd ed.. ed., New York : Oxford University Press, New York, 2000.

Gelbard, F., and Seinfeld, J. H.: The general dynamic equation for aerosols. Theory and application to aerosol formation and growth, *Journal of Colloid and Interface Science*, 68, 363-382, [https://doi.org/10.1016/0021-9797\(79\)90289-3](https://doi.org/10.1016/0021-9797(79)90289-3), 1979.

Gelbard, F., and Seinfeld, J. H.: Simulation of multicomponent aerosol dynamics, *Journal of Colloid and Interface Science*, 78, 485-501, [https://doi.org/10.1016/0021-9797\(80\)90587-1](https://doi.org/10.1016/0021-9797(80)90587-1), 1980.

Hodshire, A. L., Lawler, M. J., Zhao, J., Ortega, J., Jen, C., Yli-Juuti, T., Brewer, J. F., Kodros, J. K., Barsanti, K. C., Hanson, D. R., McMurry, P. H., Smith, J. N., and Pierce, J. R.: Multiple new-particle growth pathways observed at the US DOE Southern Great Plains field site, *Atmos. Chem. Phys.*, 16, 9321-9348, 10.5194/acp-16-9321-2016, 2016.

Kontkanen, J., Olenius, T., Lehtipalo, K., Vehkamäki, H., Kulmala, M., and Lehtinen, K. E. J.: Growth of atmospheric clusters involving cluster–cluster collisions: comparison of different growth rate methods, *Atmos. Chem. Phys.*, 16, 5545-5560, 10.5194/acp-16-5545-2016, 2016.

Kürten, A., Jokinen, T., Simon, M., Sipilä, M., Sarnela, N., Junninen, H., Adamov, A., Almeida, J., Amorim, A., and Bianchi, F.: Neutral molecular cluster formation of sulfuric acid–dimethylamine observed in real time under atmospheric conditions, *Proceedings of the National Academy of Sciences*, 111, 15019-15024, 2014.

Lehtipalo, K., Rondo, L., Kontkanen, J., Schobesberger, S., Jokinen, T., Sarnela, N., Kürten, A., Ehrhart, S., Franchin, A., Nieminen, T., Riccobono, F., Sipilä, M., Yli-Juuti, T., Duplissy, J., Adamov, A., Ahlm, L., Almeida, J., Amorim, A., Bianchi, F., Breitenlechner, M., Dommen, J., Downard, A. J., Dunne, E. M., Flagan, R. C., Guida, R., Hakala, J., Hansel, A., Jud, W., Kangasluoma, J., Kerminen, V.-M., Keskinen, H., Kim, J., Kirkby, J., Kupc, A., Kupiainen-Määttä, O., Laaksonen, A., Lawler, M. J., Leiminger, M., Mathot, S., Olenius, T., Ortega, I. K., Onnela, A., Petäjä, u., Praplan, A., Rissanen, M. P., Ruuskanen, T., Santos, F. D., Schallhart, S., Schnitzhofer, R., Simon, M., Smith, J. N., Tröstl, J., Tsagkogeorgas, G., Tome, A. n., Vaattovaara, P., Hanna Vehkama ki1, Vrtala, A. E., Wagner, P. E., Williamson, C., Wimmer, D., Winkler, P. M., Virtanen, A., Donahue, N. M., Carslaw, K. S., Baltensperger, U., Riipinen, I., Curtius, J., Worsnop, D. R., and Kulmala, M.: The effect of acid-base clustering and ions on the growth of atmospheric nano-particles, *Nature Communications*, 7, 11594, 2016.

Lehtipalo , K., Leppa , J , Kontkanen , J , Kangasluoma , J , Franchin , A , Wimnner , D , Schobesberger , S , Junninen , H , Petaja , T , Sipila , M , Mikkila , J , Vanhanen , J , Worsnop , D R & Kulmala: Methods for determining particle size distribution and growth rates between 1 and 3 nm using the Particle Size Magnifier, *Boreal Environment Research*, 19, 215-236, 2014.

Riccobono, F.: Contribution of sulfuric acid and oxidized organic compounds to particle formation and growth, *Atmos. Chem. Phys.*, 12, 9427-9439, 2012.

Riccobono, F.: Oxidation products of biogenic emissions contribute to nucleation of atmospheric particles, *Science*, 344, 717-721, 2014.

Riipinen, I., Yli-Juuti, T., Pierce, J. R., Petäjä, T., Worsnop, D. R., Kulmala, M., and Donahue, N. M.: The contribution of organics to atmospheric nanoparticle growth, *Nature Geoscience*, 5, 453, 10.1038/ngeo1499, 2012.

Smith, J., Dunn, M., VanReken, T., Iida, K., Stolzenburg, M., McMurry, P., and Huey, L.: Chemical composition of atmospheric nanoparticles formed from nucleation in Tecamac, Mexico: Evidence for an important role for organic species in nanoparticle growth, *Geophysical Research Letters*, 35, 2008.

Smith, J. N., Barsanti, K. C., Friedli, H. R., Ehn, M., Kulmala, M., Collins, D. R., Scheckman, J. H., Williams, B. J., and McMurry, P. H.: Observations of aminium salts in atmospheric nanoparticles and possible climatic implications, *Proceedings of the National Academy of Sciences*, 107, 6634-6639, 2010.

Stolzenburg, M. R., McMurry, P. H., Sakurai, H., Smith, J. N., Mauldin, R. L., Eisele, F. L., and Clement, C. F.: Growth rates of freshly nucleated atmospheric particles in Atlanta, *Journal of Geophysical Research: Atmospheres*, 110, n/a-n/a, 10.1029/2005JD005935, 2005.

Tröstl, J., Chuang, W. K., Gordon, H., Heinritzi, M., Yan, C., Molteni, U., Ahlm, L., Frege, C., Bianchi, F., Wagner, R., Simon, M., Lehtipalo, K., Williamson, C., Craven, J. S., Duplissy, J., Adamov, A., Almeida, J., Bernhammer, A.-K., Breitenlechner, M., Brilke, S., Dias, A., Ehrhart, S., Flagan, R. C., Franchin, A., Fuchs, C., Guida, R., Gysel, M., Hansel, A., Hoyle, C. R., Jokinen, T., Junninen, H., Kangasluoma, J., Keskinen, H., Kim, J., Krapf, M., Kürten, A., Laaksonen, A., Lawler, M., Leiminger, M., Mathot, S., Möhler, O., Nieminen, T., Onnela, A., Petäjä, T., Piel, F. M., Miettinen, P., Rissanen, M. P., Rondo, L., Sarnela, N., Schobesberger, S., Sengupta, K., Sipilä, M., Smith, J. N., Steiner, G., Tomè, A., Virtanen, A., Wagner, A. C., Weingartner, E., Wimmer, D., Winkler, P. M., Ye, P., Carslaw, K. S., Curtius, J., Dommen, J., Kirkby, J., Kulmala, M., Riipinen, I., Worsnop, D. R., Donahue, N. M., and Baltensperger, U.: The role of low-volatility organic compounds in initial particle growth in the atmosphere, *Nature*, 533, 527, 10.1038/nature18271, 2016.

Wang, J., McGraw, R. L., and Kuang, C.: Growth of atmospheric nano-particles by heterogeneous nucleation of organic vapor, *Atmos. Chem. Phys.*, 13, 6523-6531, 10.5194/acp-13-6523-2013, 2013.

1 Errors in Nanoparticle Growth Rates Inferred from 2 Measurements in Chemically Reacting Aerosol Systems

3 Chenxi Li¹ and Peter H. McMurry¹

4 ¹Department of Mechanical Engineering, University of Minnesota, Minneapolis, MN, 55455, USA

5

6 *Correspondence to:* Chenxi Li (lixx3838@umn.edu)

7 **Abstract.** In systems where aerosols are being formed by chemical transformations, individual particles grow due
8 to the addition of molecular species. Efforts to improve our understanding of particle growth often focus on attempts
9 to reconcile observed growth rates with values calculated from models. However, because it is typically not possible
10 to measure the growth rates of individual particles in chemically reacting systems, they must be inferred from
11 measurements of aerosol properties such as size distributions, particle number concentrations, etc. This work
12 quantifiesdiscusses errors in growth rates obtained using methods that are commonly employed for analyzing
13 atmospheric data. We analyze "data" obtained by simulating the formation of aerosols in a system where a single
14 chemical species is formed at a constant rate, R . We show that the maximum possibleoverestimation error in measured
15 growth rates occurs for collision-controlled nucleation in a single-component system in the absence of a pre-existing
16 aerosol, wall losses, evaporation or dilution, as this leads to the highest concentrations of nucleated particles. Those
17 high concentrations lead to high coagulation rates that cause the nucleation mode to grow faster than would be caused
18 by vapor condensation alone. We also show that preexisting particles, when coupled with evaporation, can
19 significantly decrease the concentration of nucleated particles. This leadscan lead to decreased discrepancies between
20 measured growth rate and true growth rate by reducing coagulation. ~~Conversely, the same concentration of~~
21 ~~preexisting~~between nucleated particles ~~has much less effect on~~. ~~However, as particle sink processes get stronger,~~
22 measured growth rates ~~during collision controlled~~can potentially be lower than true particle growth rates. We briefly
23 discuss nucleation scenarios where the observed growth rate approaches zero while the true growth rate does not.

25 **1 Introduction**

26 Aerosol systems undergo transformations by processes that include coagulation, convection, deposition on surfaces,
27 source emissions, nucleation, growth, etc. The aerosol general dynamic equation (GDE) (Friedlander, 2000;Gelbard
28 and Seinfeld, 1979, 1980) describes the time rate of change of size-dependent particle concentration and composition
29 by such processes. Recent work has focused on understanding processes that affect growth rates of freshly nucleated
30 atmospheric nanoparticles (Smith et al., 2008;Smith et al., 2010;Riipinen et al., 2012;Hodshire et al., 2016;Kontkanen
31 et al., 2016;Tröstl et al., 2016).This is important because a particle's survival probability increases with growth rates
32 (McMurtry and Friedlander, 1979;Weber et al., 1997;Kerminen and Kulmala, 2002;Kuang et al., 2010).Nucleated
33 particles are more likely to form cloud condensation nuclei and affect climate when survival probabilities are high.
34 Growth involves changesFollowing established conventions long used in modeling aerosol dynamics (Friedlander,
35 2000;Gelbard and Seinfeld, 1979, 1980),we define the sizeparticle "growth rate" as the net rate of change in diameter
36 of individual particles due to the addition or removal of molecular species.(If evaporation exceeds addition, the growth
37 rate would be negative.) While most work to date has focused on condensation and evaporation, chemical processes
38 such as acid-base reactions, organic salt formation, liquid phase reactions, and the accretion of two or more organic
39 molecules to form a larger compound having lower volatility may also contribute to growth (McMurtry and Wilson,
40 1982;Barsanti et al., 2009;Riipinen et al., 2012;Lehtipalo 2014). In a chemically reacting system, the total diameter
41 growth rate, GR , is given by the sum of all such processes:

42
$$\frac{dd_p}{dt} = GR = GR_{\text{condensation/evaporation}} + GR_{\text{acid-base reactions}} + GR_{\text{accretion}} + GR_{\text{other}}. \quad (1)$$

43 The effect of growth on the aerosol distribution function is given by (Heisler and Friedlander, 1977):

44
$$\frac{\partial n}{\partial t} \Big|_{\text{Growth}} = -\frac{\partial}{\partial d_p} \left[n(d_p, t) \frac{dd_p}{dt} \right], \quad (2)$$

45 where the aerosol number distribution, $n(d_p, t)$ is defined such that the number concentration of particles between d_p
46 and $d_p + dd_p$ is equal to $n(d_p, t)dd_p$. Coagulation, including the coagulation of a molecular cluster with a larger
47 particle, can also lead to particle growth. It is worthwhile, however, to treat coagulation and growth separately. The
48 extent to which the coagulation of freshly nucleated molecular clusters contributes to measured growth rates can be
49 accurately determined only if the entire number distribution down to clusters of size 2 is accurately measured. In the
50 absence of such data, the contributions of cluster coagulation to growth could erroneously be attributed to vapor uptake.

51 Coagulation is accounted for with the coagulation integrals in the GDE and is a relatively well understood process
52 that can be described with reasonable confidence in models (Kürten et al., 2018;Chan and Mozurkewich, 2001).
53 Growth involves processes that are not well understood for chemically complex aerosol systems, such as the
54 atmosphere (Barsanti et al., 2009;Riipinen et al., 2012;Hodshire et al., 2016).

55 Progress towards understanding growth can be achieved through efforts to reconcile GRs that are observed
56 experimentally with values predicted by models. Such work requires that size- and time-dependent GRs be accurately
57 determined from observations. The literature includes many reports of observed GRs (Stolzenburg et al., 2005;Wang
58 et al., 2013;Riccobono, 2012;Tröstl et al., 2016), but uncertainties in reported values are typically not well understood.

59 Because it is usually not possible to measure the growth of individual particles as they undergo chemical
60 transformations, GRs are calculated indirectly using time-dependent observations of aerosol properties such as number
61 distributions or number concentrations larger than a given size. Those properties are typically affected by many
62 processes, some poorly understood, that can affect reported GRs to an unknown extent.

63 A variety of approaches have been used to extract GRs from observations. We refer to these values as GR_m , where the
64 subscript ‘m’ designates ‘measured’. Methods that we discuss include:

65 1. *Maximum Concentration Method* (Kulmala et al., 2012). During a nucleation event, particle concentrations in
66 a given size bin increase from their initial values, passing through a peak before they eventually decrease. This
67 technique involves noting the times that this maximum occurred in ~~two~~-different size bins. The growth rate is
68 ~~then assumed equal obtained by first fitting a linear function of particle diameter (corresponding~~ to the
69 ~~difference in bin size divided by the difference in bins) vs.~~ time, ~~and then calculating the slope of the fitted~~
70 ~~function.~~

71 2. *Appearance Time Method* (Lehtipalo 2014). This approach has been used ~~primarily~~ to analyze data from
72 condensation particle counter (CPC) batteries (Riccobono, 2014), particle size magnifier (PSM) (Lehtipalo
73 2014), etc. In brief, GR_m is determined by the differences in concentration rise times (typically, either 5% or
74 50% of the maximum) measured by EPCs the instruments with differing minimum detection sizes. A variation
75 of this approach was reported by Weber et al. (1997), who estimated growth rates from the observed time delay
76 in measurements of sulfuric acid vapor and particles measured with a condensation particle counter having a
77 minimum detectable size of about 3 nm.

78 3. *Log-normal Distribution Function Method* (Kulmala et al., 2012). Lognormal distributions are fit to the
79 growing mode of nucleated particles. GR_m is defined as the growth rate of the geometric mean size of these
80 distributions.

81 While these methods do not account for the effects of coagulation on measured changes in particle size, the literature
82 includes approaches that explicitly account for such effects (Lehtinen et al., 2004; Verheggen and Mozurkewich,
83 2006; Kuang et al., 2012; Pichelstorfer et al., 2017). Other work has applied the above techniques after confirming that
84 coagulation has an insignificant effect for the analyzed data (Kulmala et al., 2012) or explicitly accounting for the
85 effects of coagulation on GR_m (Stolzenburg et al., 2005; Lehtipalo et al., 2016).

86 ~~Recent work has focused on understanding processes that affect GR of freshly nucleated atmospheric nanoparticles.~~
87 ~~This is important because a particle’s survival probability increases with GR. Nucleated particles are more likely to~~
88 ~~form cloud condensation nuclei and affect climate when survival probabilities are high.~~ This paper assesses errors of
89 using GR_m calculated using techniques commonly employed in the literature-to infer particle growth rates. Our results
90 are especially germane to GR of freshly nucleated particles ranging in size from molecular clusters to about 40 nm.
91 We use time-dependent distribution functions calculated numerically by McMurry and Li (2017) as “data”. The only
92 process contributing to the addition or removal of molecular species in that work (i.e., to particle “growth rates” as is
93 defined above) are condensation and evaporation. ~~We do not examine errors associated with convection, source~~

94 ~~emission, etc.~~ Because we understand this model system perfectly, ~~true particle growth rates (GR_{true} (i.e., the net~~
95 ~~growth rate due molecular exchange through condensation and evaporation)~~ can be calculated exactly. Errors in GR_m
96 ~~due to coagulation, wall deposition, scavenging by preexisting particles, or dilution,~~ are given by the difference

97 between GR_{true} and GR_m . ~~We do not examine errors associated with convection, source emission, etc.~~

98 We are not the first to examine factors that cause GR_m to differ from GR_{true} . For example, Kontkanen (2016) used
99 simulations to show that discrepancies between ~~GR_m and GR_{true} can be significant. measured growth rate based on~~
100 ~~appearance time (AGR) and growth rate based on irreversible vapor condensation (CGR) can be significant. (Note~~
101 ~~GR_{true} used in this paper differs from CGR in that GR_{true} also incorporates evaporation.)~~ Our approach, which uses the
102 non-dimensional formulation described by McMurry and Li (2017), provides results that are generally applicable to
103 nucleation and growth of a single chemical species, so long as it is being produced by chemical transformations at a
104 constant rate, R . We show that the upper limit for ~~errors in overestimation of GR_{true} by GR_m~~ occurs when nucleation
105 takes place in the absence of pre-existing aerosols and is collision-controlled (i.e., when evaporation rates from even
106 the smallest clusters occur at rates that are negligible relative to vapor condensation rates). Collision-controlled
107 nucleation is an important limiting case because there is growing evidence that atmospheric nucleation of sulfuric acid
108 with stabilizing species is well-described as a collision-controlled process (Almeida et al., 2013; Kürten et al.,
109 2018; McMurry, 1980). Because cluster evaporation, scavenging by preexisting aerosol, etc., all diminish the number
110 of particles formed by nucleation, ~~errors in GR_m overestimation of GR_{true} due to coagulation decreases~~ as these
111 processes gain in prominence. We do not explicitly study the effect of growth by processes other than condensation
112 or evaporation, such as heterogeneous growth pathways that take place on or within existing particles. If such
113 processes were to contribute significantly to growth, they would lead to higher growth rates and therefore smaller
114 relative errors in GR_m due to coagulation. ~~Additionally, we point out when particle sink processes consume nucleated~~
115 ~~particles at a fast rate (e.g. strong effects of dilution or scavenging by preexisting particles), GR_m may not be used to~~
116 ~~estimate GR_{true} . Our results help to inform estimates of uncertainties for systems with a single condensing species, or~~
117 ~~systems that can be modeled in a similar way to a single species system~~ (Kürten et al., 2018) ~~Our results help to inform~~
118 ~~estimates of uncertainty for complex aerosol systems, such as the atmosphere, where errors are difficult to quantify.~~

119 2 Methods

120 2. 1 Discrete-sectional model

121 We utilize the dimensionless discrete-sectional model described by McMurry and Li (2017) to simulate evolution of
122 particle size distribution for a system with a single condensing species. We assume that the condensing species is
123 produced at a constant rate by gas phase reaction. Our code uses two hundred discrete bins and 250 sectional bins,
124 with a geometric volume amplification factor of 1.0718 for neighboring sections.

125 Physical processes that affect particle growth, including wall deposition, loss to pre-existing particles, cluster
126 evaporation and dilution, can be characterized by dimensionless parameters in this model. In the present study,
127 however, not all aforementioned processes are discussed. Our previous work shows that wall losses, scavenging by

128 preexisting particles and dilution have qualitatively similar effects on aerosol dynamics. Therefore, in this work we
 129 focus on preexisting aerosols and dilution to illustrate factors that contribute to errors in measured growth rates, and
 130 do not explicitly discuss wall deposition or dilution. A single dimensionless parameter, \sqrt{L} , is used to indicate the
 131 abundance of preexisting particles, with larger \sqrt{L} representing higher concentration of preexisting particles (or,
 132 equivalently, a slower rate at which the nucleating species is produced by chemical reaction). \sqrt{L} is calculated with
 133 the equation

$$134 \quad \sqrt{L} = \frac{\frac{1}{4} \left(\frac{8k_b T}{\pi m_1} \right)^{1/2} A_{Fuchs}}{\sqrt{R \beta_{fm} 11}} \quad (3)$$

135 where A_{Fuchs} is the Fuchs surface area concentration (Fuchs and Sutugin, 1971)in addition, k_b is the Boltzmann

136 constant, m_1 is the mass of the monomer, R is the condensing species production rate, $\beta_{11 fm}$ is the monomer collision

137 frequency function. The loss rate for particles containing k monomers is $\sqrt{L}/k^{1/2}$. This size dependence is included

138 when solving the coupled differential equations for time-dependent cluster concentrations. Similarly, the

139 dimensionless quantity M that characterizes dilution is given by the expression

$$140 \quad M = \frac{Q_{dil}/V}{\sqrt{R \beta_{fm} 11}}, \quad (4)$$

141 where Q_{dil} is the dilution flow rate and V is the volume of the system. Note the fractional dilution loss is independent
 142 of particle size. In addition to loss to pre-existing particles and dilution, we consider the effect of cluster evaporation
 143 on particle growth with the assumption that evaporation follows the classical liquid droplet model. Two dimensionless
 144 parameters, E and Ω , are needed to fully describe the evaporation process. The dimensionless evaporation parameter,
 145 E , is proportional to the saturation vapor concentration of the nucleating species, while Ω is the dimensionless surface
 146 tension (Rao and McMurry, 1989; McMurry and Li, 2017). The evaporation rate for particles containing k monomers,
 147 E_k , is calculated with a discretized equation of the form:

$$148 \quad E_k = E c_{1k} \exp \left[\frac{3}{2} \Omega \left(k^{\frac{2}{3}} - (k-1)^{\frac{2}{3}} \right) \right], \quad (5)$$

149 where $c(i, k)$ is the dimensionless collision frequency between a monomer and a particle containing k monomers. To
 150 simplify our discussion, Ω is fixed to be 16 throughout this work (a representative value for the surface tension of
 151 sulfuric acid aqueous solutions), while the value of E is varied.

152 The solution to the GDE for a constant rate system ($R=\text{constant}$) depends on dimensionless time, cluster size and the
 153 dimensionless variables \sqrt{L} , M , E , Ω , etc., but is independent of the rate at which condensing vapor is produced by
 154 chemical reaction. That rate is required to transform the computed nondimensional solutions to dimensional results
 155 using simple multiplicative expressions given by McMurry and Li (2017):

$$156 \quad N_k = \left(\frac{R}{\beta_{11 fm}} \right)^{1/2} \tilde{N}_k; \quad t = \left(\frac{1}{R \beta_{11 fm}} \right)^{1/2} \tau; \quad d_p = (v_1^{1/3}) \tilde{d}_p. \quad (36)$$

157 In the above equations, R is the condensing species production rate, $\beta_{11, fm}$ is the free molecular collision frequency
 158 between 2 monomers, \tilde{N}_k is the dimensionless concentration of particle containing k monomers, τ is the dimensionless
 159 time, \tilde{d}_p is the dimensionless particle size and v_1 is the monomer volume. Assuming a monomer volume of
 160 $1.62 \times 10^{-22} \text{ cm}^3$ (volume of one sulfuric acid plus one dimethylamine molecule with a density of 1.47 g/cm^3), $\tilde{d}_p =$
 161 30 would be equivalent to a dimensional particle size of 16.4 nm.

162 **2.2 Evaluation of measured growth rate (GR_m)**

163 At time t_1 and t_2 , if two particle sizes $d_{p,t1}$ and $d_{p,t2}$ are used to represent the particle size distribution, the ‘measured’
 164 growth rate can be calculated using the following equation as a first order approximation

$$165 GR_m\left(\frac{d_{p,t_1}+d_{p,t_2}}{2}, \frac{t_2+t_1}{2}\right) = \frac{d_{p,t_2}-d_{p,t_1}}{t_2-t_1}. \quad (47)$$

166 If d_{p,t_i} is available for a time series $\{t_i\}_{i=1,2,\dots}$, growth rate can also be obtained by derivatizing a fitting function
 167 $d_p = d_p(t)$ to obtain growth rate at any time t_a :

$$168 GR_m(d_p, t_a) = \left. \frac{dd_p(t)}{dt} \right|_{t=t_a}. \quad (58)$$

169 To implement Eq. (47) or (58), it is necessary to choose a particle size that is representative of the particle size
 170 distribution at a given time. The choice of this representative size varies among publications and can depend on the
 171 types of available data. Based on previous studies (Kulmala et al., 2012; Lehtipalo 2014; Stolzenburg et al., 2005; Yli-
 172 Juuti, 2011), we have selected four representative sizes for discussion: $\tilde{d}_{p,mode}$, $\tilde{d}_{p,sr100}$, $\tilde{d}_{p,sr50}$ and $\tilde{d}_{p,tot50}$. At a
 173 given time τ , $\tilde{d}_{p,mode}$ is the particle size at which $d\tilde{N}(\tau)/d\log_{10}\tilde{d}_p$ reaches its local maximum. If the shape of the
 174 mode is log-normal, $\tilde{d}_{p,mode}$ is equal to the geometric mean of the distribution. As suggested by Kulmala et al.
 175 (Kulmala et al., 2012), the ‘log-normal distribution method’ involves calculating growth rates from observed time-
 176 dependent trends of $\tilde{d}_{p,mode}$. The ‘maximum concentration method’ is based on the time when particles in a given
 177 size bin, $\tilde{d}_{p,sr100}$, pass through their maximum (100%) concentration (Lehtinen and Kulmala, 2003). The ‘appearance
 178 time’ method is based on the time when particle concentrations in a bin, $\tilde{d}_{p,sr50}$, pass through a specified percentage
 179 of its maximum (we have used 50%). Growth rates are sometimes based on total concentrations of particles larger
 180 than a specified size. We refer to the particle size above which the total number concentration of particles reaches 50%
 181 of its maximum value as $\tilde{d}_{p,tot50}$. This approach is especially useful when measurements are carried out with a battery
 182 of CPCs having differing cutoff sizes. For simplicity, in this paper we assume that CPC detection efficiencies increase
 183 from 0% to 100% at a given cutoff size. In practice, measured size-dependent detection efficiencies are typically used
 184 when analyzing CPC battery data. Figure 1 shows the location of these representative sizes at $\tau = 20, 60, 100$ for two
 185 nucleation scenarios in the absence of preexisting particles. $\tilde{d}_{p,mode}$, $\tilde{d}_{p,sr100}$, $\tilde{d}_{p,sr50}$ and $\tilde{d}_{p,tot50}$ are marked as
 186 points, with their y-coordinates representing particle concentrations at corresponding sizes.

187 As will be shown later, values of GR_m obtained with $\tilde{d}_{p,mode}$, $\tilde{d}_{p,sr100}$, $\tilde{d}_{p,sr50}$ or $\tilde{d}_{p,tot50}$ are not equal. To
 188 differentiate these cases, GR_m are notated as $GR_{m,mode}$, $GR_{m,sr100}$, $GR_{m,sr50}$ and $GR_{m,tot50}$ accordingly.

189 **2.3 Evaluation of true growth rate (GR_{true})**

190 The true ~~net~~ growth rate (GR_{true}) ~~defined in this paper follows the Lagrangian approach~~ (Olenius et al., 2014) GR_{true} ,
 191 ~~due to molecular, i.e. tracking the volume change of individual particles, and only include molecular species exchange~~
 192 ~~by condensation and evaporation. It~~ is calculated with the following expression:

$$193 GR_{true} = \frac{d\tilde{d}_p}{d\tau} = \frac{2}{\pi\tilde{d}_p^2} \frac{d\tilde{V}}{d\tau} = \frac{2}{\pi\tilde{d}_p^2} \cdot \frac{\tilde{V} + c(i,k)\tilde{N}_1 \cdot d\tau - E_k \cdot d\tau - \tilde{V}}{d\tau} = \frac{2(c(i,k)\tilde{N}_1 - E_k)}{\pi\tilde{d}_p^2}, \quad (69)$$

194 where \tilde{d}_p is the representative size, \tilde{N}_1 is the concentration of monomers, ~~$c(i,k)$ is the collision frequency between~~
 195 ~~monomers and particles of size \tilde{d}_p (containing k monomers)~~, and E_k is the particle ~~the~~ evaporation rate. ~~Assuming~~
 196 ~~cluster evaporation follows the liquid droplet model, E_k is calculated with a discretized equation of the form: given~~
 197 ~~by Eq. (5).~~

198 If evaporation is negligible ($E = 0$) and \tilde{N}_1 is constant, Eq. (69) leads to a higher growth rate for smaller particles,
 199 mainly because of the increased monomer collision frequency relative to particle size (Tröstl et al., 2016). Throughout
 200 this work Eq. (69) is used to evaluate true particle growth rate. Note GR_{true} is calculated from dimensionless size and
 201 time, and is therefore dimensionless. Since we focus on relative values of true and measured growth rates, our
 202 conclusions are unaffected by the dimensionality of GR . However, dimensionless growth rates can be converted to
 203 dimensional values with Eq. (36).

204 **3. Results and discussion**

205 **3.1 Error of using $GR_{m,mode}$ as GR_{true}**

206 As mode diameter ($\tilde{d}_{p,mode}$) is often employed to derive particle growth rate, in this section we discuss the error of
 207 using $GR_{m,mode}$ as a substitute for GR_{true} in the absence of preexisting particles. The effect of preexisting particles is
 208 discussed in Sect. 3.3.

209 Both condensation and coagulation lead to growth of $\tilde{d}_{p,mode}$. To understand their relative importance, we attribute
 210 $GR_{m,mode}$ to three processes: monomer condensation minus evaporation (GR_{true}), coagulation of the mode with clusters
 211 ($GR_{m,cluster}$) and self-coagulation of the mode ($GR_{m,self}$). The latter two processes are the main causes of the discrepancy
 212 between $GR_{m,mode}$ and GR_{true} . To evaluate $GR_{m,cluster}$ and $GR_{m,self}$, the range of ‘clusters’ and ‘mode’ are defined as
 213 illustrated in Fig. 1 by the two shaded regions at $\tau = 100$: clusters (beige) and nucleation mode (light blue). Clusters
 214 and nucleation mode are separated by $\tilde{d}_{p,min}$, where $d\tilde{N}/d\log_{10}\tilde{d}_p$ is at a local minimum. Stolzenburg et al. (2005)
 215 assumed the nucleation mode is lognormal and calculated GR_{true} and $GR_{m,self}$ with the method of moments. In this
 216 work, since the mode for collision-controlled nucleation deviates significantly from log-normal (see Fig. 1a), no
 217 assumption regarding the shape of the nucleation mode is made. Instead, $GR_{m,cluster}$, $GR_{m,self}$ are calculated with the
 218 first order numerical approximation method outlined in Appendix A.

219 The calculation results are summarized by Fig. 2. We first consider collision-controlled nucleation ($E=0$). For this
 220 nucleation scenario, Fig. 2a shows $\tilde{d}_{p,mode}$ on the left y axis and growth rate values on the right. A third order

221 polynomial is used for fitting $\tilde{d}_{p,mode} = \tilde{d}_{p,mode}(\tau)$ and is plotted as a solid black line. Differentiating the fitted
222 polynomial with respect to time gives the value of $GR_{m,mode}$. It is clear that GR_{true} only accounts for a small fraction
223 (17%-20%) of GR_m and is on par with contribution of $GR_{m,cluster}$ (15%-22%). Self-coagulation is the major contributor
224 (62%-78%) to GR_m . Thus, using $GR_{m,mode}$ as a substitute for GR_{true} leads to an overestimation by as much as a factor
225 about 6. We believe collision-controlled nucleation ($E=0$) in the absence of other particle loss mechanisms such as
226 wall deposition ($W=0$) and scavenging by pre-existing particles ($\sqrt{L}=0$) provides an upper limit to errors in GR_m for
227 overestimation of GR_{true} for a constant rate system ($R=\text{constant}$). This is because these conditions lead to the maximum
228 number of particles that can be produced by nucleation. High concentrations lead to high coagulation rates, and it is
229 coagulation that is primarily responsible for errors in GR_m . Furthermore, as is discussed below, the absence of
230 evaporation and scavenging by nucleated particles keeps monomer concentrations low relative to values achieved
231 when $E \neq 0$ (see Fig. 2a). Low monomer concentrations reduce the value of GR_{true} , thereby increasing relative errors in
232 GR_m .

233 Distinctive features of particle growth emerge when cluster evaporation is included by setting $E = 1 \times 10^{-3}$. Figure
234 2b shows results for this nucleation scenario. Most noticeably, particles grow considerably faster at early stages of
235 simulation. This occurs because evaporation depletes clusters and correspondingly increases monomer concentration.
236 In the absence of pre-existing particles, monomer concentration accumulates until the supersaturation is high enough
237 for nucleation to take place (see figure 2c). The accumulated monomers then rapidly condense on the nucleated
238 particles, leading to the rapid particle growth shown in figure 2b. To capture this rapid growth, two third-order
239 polynomials are used to fit $\tilde{d}_{p,mode}$ values for $\tau < 40$ and $\tau > 35$ respectively, with an overlapping region for $35 <$
240 $\tau < 40$. Furthermore, in comparison to collision-controlled nucleation, contribution of $GR_{m,cluster}$ to $GR_{m,mode}$ becomes
241 negligible, due to decreased cluster concentration by evaporation. For $\tau > 30$, GR_{true} accounts for about 40%-55% of
242 $GR_{m,mode}$, larger than that of collision-controlled nucleation; for $\tau < 25$, GR_{true} almost entirely accounts for $GR_{m,mode}$
243 and even exceeds $GR_{m,mode}$ at the very beginning of the nucleation. $GR_{true}/GR_{m,mode} > 1$ indicates a rapidly forming
244 nucleation mode, where freshly nucleated particles enter the mode and skew the mode distribution toward smaller
245 sizes, slowing down the shift of the mode peak towards larger values.

246 Increase of $GR_{true}/GR_{m,mode}$ by evaporation is explained by the elevated monomer concentration due to particle
247 volatility and the smaller number of particles formed by nucleation: the former increases GR_{true} , and the latter decreases
248 $GR_{m,self}$ and $GR_{m,cluster}$. Figure 2c plots monomer concentration \tilde{N}_1 as a function of time for several values of E .
249 Noticeably, monomer concentration elevates with E since higher cluster evaporation rates require higher monomer
250 concentrations (i.e., higher supersaturation) to overcome the energy barrier of nucleation. Once nucleation takes place,
251 high monomer concentration leads to rapid nanoparticle growth rates.

252 Figure 2d shows $GR_{true}/GR_{m,mode}$ at $\tau = 30, 50, 100, 150$ for several E values. At a given time, $GR_{true}/GR_{m,mode}$ clearly
253 increases with E : when evaporation rates are not negligible (i.e., $E \neq 0$), $GR_{m,mode}$ is closer to GR_{true} than occurs when
254 $E=0$. Again, this is because the elevated monomer concentrations increase GR_{true} and the lowered concentrations of
255 clusters and nucleated particles decrease $GR_{m,cluster}$ and $GR_{m,self}$. As E approaches 0, the value of $GR_{true}/GR_{m,mode}$
256 converges to that of the collision-controlled nucleation (~ 0.2). One data point, corresponding to $E = 5 \times 10^{-3}$ and

257 $\tau = 30$, with a value of 1.8, is not shown in Fig. 2d. It has a value significantly greater than unity because of the large
258 quantities of nucleated particles entering the mode, skewing the mode peak toward smaller sizes.

259 **3.2 Comparison of representative sizes**

260 In this section we examine how observed growth rate depends on the choice of a representative size. The application
261 of $GR_{m,mode}$ to deduce GR_{true} , though convenient in practice, depends on the existence of a nucleation mode. However,
262 the nucleation mode is usually not well defined in the early stage of nucleation. In contrast, growth rate based on other
263 representative sizes ($\tilde{d}_{p,sr50}$, $\tilde{d}_{p,sr100}$ and $\tilde{d}_{p,tot50}$) are not dependent on mode formation and are available for all
264 particle sizes. In light of this, $GR_{m,sr100}$, $GR_{m,sr50}$, $GR_{m,tot50}$ have often been employed to describe the growth rate of
265 small particles (<5nm). The effects of pre-existing particles are neglected in this section (i.e., $\sqrt{L} = 0$) but are
266 discussed in Sect. 3.3.

267 For collision-controlled nucleation, $\tilde{d}_{p,mode}$, $\tilde{d}_{p,sr50}$, $\tilde{d}_{p,sr100}$, $\tilde{d}_{p,tot50}$ are plotted as functions of time in Fig. 3a. The
268 magnitude of the representative sizes follow $\tilde{d}_{p,mode} < \tilde{d}_{p,bin100} < \tilde{d}_{p,tot50} < \tilde{d}_{p,bin50}$, as was previously illustrated in
269 Fig. 1a. $\tilde{d}_{p,mode} < \tilde{d}_{p,bin100}$ indicates that a certain measurement bin first reaches its maximum concentration and
270 becomes a local maximum at a later time. This is true for collision-controlled nucleation with a decreasing peak
271 concentration but is not necessarily true for other nucleation scenarios. The observed growth rate (i.e. slope of curves
272 in Fig. 3a) are shown in Fig. 3b as a function of representative size, with a clear relationship $GR_{m,mode} < GR_{m,sr100}$
273 $< GR_{m,tot50} < GR_{m,sr50}$. Note that $GR_{m,mode}$ is not available for small sizes, indicating the nucleation mode is yet to form
274 at the early stage of nucleation. Figure 3c shows GR_{true}/GR_m as a function of representative size, with GR_{true} calculated
275 with Eq. (69). Clearly GR_{true} accounts for the highest percentage of GR_m at the start of nucleation. This is partly due
276 to higher monomer concentrations (see red solid curve in Fig. 2c) and partly due to Eq. (69) that leads to higher true
277 growth rate for smaller particles: the addition of a monomer leads to a bigger absolute as well as fractional diameter
278 growth for small particles.

279 Figure 3d-3f are counterparts of Fig. 3a-3c, but with evaporation constant E set to 1×10^{-3} . Figure 3d shows rapid show
280 that $\tilde{d}_{p,sr50}$ and $\tilde{d}_{p,tot50}$ increase of representative size with time at the start of nucleation, but a careful examination
281 of clusters containing a few monomers reveals they grow relatively slowly at the start of the simulation (see the
282 amplified figure at the lower right corner of Fig. 3a-3d; for reference, the dimensionless sizes of monomer, dimer and
283 trimer are 1.24, 1.56 and 1.79 respectively). Subsequently, a marked change slope of the $\tilde{d}_p = \tilde{d}_p(\tau)$ curve is observed,
284 indicating accelerated particle growth. This reflects that nucleation occurs with a burst of particle formation following
285 a process of monomer and cluster accumulation. The slow growth of the smallest clusters is an indication that the
286 accumulation process is ‘slow’ slow due to the strength of the Kelvin effect.

287 Figure 3e shows GR_m obtained by curve fitting after the nucleation burst and Fig. 3f shows the corresponding
288 GR_{true}/GR_m values. Different from collision-controlled nucleation, there is a sharp rise of GR_{true}/GR_m value at the start
289 of nucleation. This is due to the sharp decrease of the evaporation term in Eq. (69), causing the value of GR_{true} to
290 increase sharply. As nucleation progresses, the ratio of GR_{true} to $GR_{m,sr100}$, $GR_{m,tot50}$ and $GR_{m,sr50}$ comes close to 1,

291 with $GR_{m,mode}$ not yet available. Eventually, GR_{true}/GR_m for all representative sizes decreases and fall into the range
292 of 30%-50%, with GR_m^{mode} giving the best estimate of GR_{true} . Note the value of $GR_{true}/GR_{m,mode}$ significantly
293 exceeds unity for $\tilde{d}_p \in [10, 15, 5, 11]$ due to the distortion of the mode toward smaller sizes by high flux of freshly
294 nucleated particles into the mode.

295 **3.3 Effect of pre-existing particles**

296 Pre-existing particles act as particle sinks to decrease the intensity of nucleation. Similarly, in chamber experiments,
297 though loss to pre-existing particles is often eliminated by using air that is initially particle-free, loss of particles to
298 chamber walls is inevitable. Since wall loss and loss to preexisting particles have qualitatively similar effect on
299 nucleation (McMurry and Li, 2017), we selectively examine the effect of preexisting particles on growth rate
300 measurements to qualitatively illustrate the effects of all of these processes. To probe the initial stage of nucleation,
301 we use $\tilde{d}_{p,bin50}$ as the basis for our analysis, with a comparison of representative sizes presented at the end of this
302 section. As to the magnitude of \sqrt{L} , we choose $\sqrt{L} \in [0, 0.3]$ based on previous work. It was shown in Fig. 2b in
303 McMurry and Li (2017) that as \sqrt{L} exceeds 0.1, particle size distributions begin to deviate discernably from the
304 collision-controlled case. In addition, $\sqrt{L} \approx 0.2$ was observed in the ANARChE field campaign carried out in Atlanta
305 for nucleation events with sulfuric acid as the major nucleating species (Kuang et al., 2010).

306 The influence of preexisting particles on the discrepancy between true and measured growth rate (GR_{true}/GR_m) is
307 twofold. On one hand, preexisting particles can decrease monomer concentration which leads to a smaller GR_{true} . On
308 the other hand, preexisting particles reduce coagulation by scavenging nucleated particles, which could result in a
309 narrower gap between GR_{true} and GR_m . Therefore, the response of GR_{true}/GR_m to \sqrt{L} depends on the relative magnitude
310 of these two competing effects. Figure 4a shows $\tilde{d}_{p,sr50}$ as a function of time for several \sqrt{L} values and Fig. 4b displays
311 the corresponding GR_{true}/GR_m values. It can be seen that GR_{true}/GR_m positively correlates with \sqrt{L} , indicating
312 preexisting particles are more effective in removing nucleated particles than reducing monomer concentrations. In
313 fact, as further demonstrated by Fig. 4c, monomer concentrations (leftmost point of all the curves) are barely affected:
314 scavenging of monomers by preexisting particles are offset by less condensation of monomers onto nucleated particles.
315 Note that for the range of \sqrt{L} values examined, the presence of preexisting particles alter GR_{true}/GR_m values by no
316 more than 50%-% for collision-controlled nucleation.

317 Figures 4d-4f show the same quantities as are shown in Fig. 4a-4c, but with E set to 1×10^{-3} instead of zero. In
318 contrast to collision-controlled nucleation, pre-existing particles significantly affect the nucleation process when
319 cluster evaporation is taken into account. As \sqrt{L} increases, Fig. 4e shows GR_{true}/GR_m converges to a value slightly
320 larger than unity. This indicates that the contribution of coagulation to measured growth rate approaches zero as \sqrt{L}
321 becomes large; or equivalently, the concentration of nucleated particles is severely decreased by pre-existing particles.
322 Values of $GR_{true}/GR_{m,sr50}$ slightly exceed unity for large sizes (Fig. 4f) due to the slightly higher condensational growth
323 rates of smaller particles in the nucleation mode. This shifts values of $\tilde{d}_{p,sr50}$ towards smaller sizes than would occur
324 if all particles were to grow at the same rate, causing $GR_{m,sr50}$ to be smaller than GR_{true} .

325 The decrease of nucleated particle concentration is further demonstrated in Fig. 4f. From $\sqrt{L} = 0$ to $\sqrt{L} = 0.3$, the
326 peak concentration of nucleated particles dropped by about three orders of magnitude. Such a decrease in concentration
327 of nucleated particles results from the limiting effect of \sqrt{L} on monomer concentration ~~at the moment of the~~
328 ~~nucleation burst.~~ If pre-existing particles are absent, then no major loss mechanisms for monomers exist prior to ~~the~~
329 nucleation burst. Monomer would accumulate until the nucleation energy barrier can be overcome: the higher the
330 energy barrier, the higher the monomer concentration ~~accumulates prior~~ to ~~be (nucleation, as)~~ shown in Fig. 2c~~).~~ The
331 elevated monomer concentration then leads to rapid growth of freshly nucleated particles ~~right after~~~~immediately~~
332 ~~following the~~ nucleation burst. However, in the presence of pre-existing particles (i.e., $\sqrt{L} \neq 0$), monomer
333 concentration can only increase to the point where its production and consumption by preexisting particles reach
334 balance, prohibiting its concentration from reaching a high value even prior to ~~nucleation burst~~~~the nucleation burst.~~
335 ~~To facilitate comparison with experimental results, in Appendix B we provide an example of conversion from~~
336 ~~dimensionless distributions and growth rates to dimensional ones.~~

337 Finally, Fig. 5 examines the difference between representative sizes used to calculate GR_m when loss to preexisting
338 particles is accounted for. Two cases are presented: (1) collision-controlled nucleation ($E=0$) with $\sqrt{L} = 0.2$ (Fig. 5a-
339 5c) and (2) nucleation accounting for both cluster evaporation and scavenging by preexisting particles ($E =$
340 1×10^{-3} and $\sqrt{L} = 0.2$; Fig. 5d-5f). For collision-controlled nucleation with $\sqrt{L} = 0.2$, the preexisting particles
341 changes nucleation only slightly, although GR_m decreases and GR_{true}/GR_m increases both to a minor extent compared
342 to collision-controlled nucleation in the absence of a preexisting aerosol (compare Fig. 5a-5c to Fig. 3a-3c). The
343 analysis made in the discussion of Fig. 3a-3c still stands for Fig. 5a-5c. For nucleation with evaporation and preexisting
344 particles coupled together, ~~two (Fig. 5d-5f), three~~ features are worthy of attention. Firstly, compared to evaporation-
345 only nucleation, GR_m is significantly decreased for small particle sizes. For $\tilde{d}_p < 10$, GR_m is no larger than 0.7 with
346 preexisting particles but can be greater than 1.5 without (refer to Fig. 3e). Secondly, as shown in Fig. 5f, $GR_{true}/GR_{m,sr50}$
347 and $GR_{true}/GR_{m,tot50}$ comes close to unity ~~for all representative sizes~~ due to negligible coagulation effects. ~~Third,~~
348 $GR_{true}/GR_{m,mode}$ is between 1.2 and 1.5 and $GR_{true}/GR_{m,sr100}$ is between 1.1 and 1.2 for $\tilde{d}_p > 10$, ~~indicating the true~~
349 ~~growth will be slightly underestimated if $\tilde{d}_{p,mode}$ or $\tilde{d}_{p,sr100}$ are used to infer GR_{true} .~~

350 3.4 Underestimation of GR_{true}

351 In ~~previous sections, mainly overestimation of the GR_{true} by measured growth rate, GR_m , has been discussed. Though~~
352 ~~we do no quantitatively study underestimation of GR_{true} by GR_m , in this section we show that in a constant rate system~~
353 ~~where particle sink processes (i.e. dilution and loss to pre-existing particles) strongly decrease the concentration of~~
354 ~~nucleated particles, GR_m can approach zero and cannot be utilized to estimate GR_{true} . Figure 6 shows such~~ nucleation
355 ~~scenarios for (a) collision-controlled nucleation with $M = 0.1$ and (b) collision-controlled nucleation with $\sqrt{L} = 1.5$.~~
356 ~~In both cases other sink processes were set equal to zero. As shown in both Fig. 6a and 6b, particle size distributions~~
357 ~~approach steady state after $\tau = 100$. As a result, the measured growth rate GR_m approaches zero beyond $\tau = 100$. At~~

358 the same time, true condensational growth remains finite since monomer concentration remains steady state after $\tau =$
359 20. Therefore, other methods have to be utilized to infer GR_{true} in such situations.

360

361 4 Conclusions

362 We used a discrete-sectional model to solve a dimensionless form of aerosol population balance equation for a single-
363 species system. True growth rate and various “measured” growth rates were examined for a variety of nucleation
364 scenarios. Based on the simulation results, we draw the following conclusions:

- 365 1. Simulated data shows that for collision-controlled nucleation without preexisting particles ~~results in an upper~~
366 ~~limit (up to a factor, growth rates inferred from the modal size of 6) to discrepancies between true (GR_{true})~~
367 ~~and measured (e.g., nucleated particles ($GR_{m,mode}$) growth rates is as much as 6 times greater than true growth~~
368 ~~rates due to vapor condensation (GR_{true}).~~
- 369 2. In the absence of preexisting particles or other sink processes, comparison of different growth rates based on
370 different representative sizes indicates the relationship $GR_{m,mode} < GR_{m,sr100} < GR_{m,tot50} < GR_{m,sr50}$ holds true for
371 collision-controlled nucleation. If clusters evaporate, the nucleation process is characterized by rapid particle
372 growth following the nucleation burst.
- 373 3. Both evaporation and scavenging by preexisting particles ~~bring GR_{true}/GR_m closer to unity by decreasing can~~
374 ~~reduce the number concentration of nucleated particles. In formed by nucleation. Lower particle~~
375 ~~concentrations reduce the ease effect of evaporation, GR_{true}/GR_m also increases as a result coagulation on GR_m ,~~
376 ~~so overestimation of elevated monomer concentration GR_{true} by GR_m is lower than is found in the absence of~~
377 ~~these processes.~~
- 378 4. Preexisting particles have dramatically different effects on collision-controlled nucleation and nucleation
379 with cluster evaporation. For $\sqrt{L} \in [0,0.3]$, collision-controlled nucleation is only slightly affected. However,
380 if preexisting particles are coupled with evaporation, the number of nucleated particles can drop significantly.
381 ~~In this case, GR_m based on all representative sizes can be a good approximation of GR_{true} due to negligible~~
382 ~~coagulation effects, thus reducing the contribution of coagulation to measure growth rates.~~
- 383 4.5. GR_m can underestimate GR_{true} in a system with strong dilution or other particle sink processes. Particle size
384 distributions in such nucleation scenarios can approach a steady state that leads to a GR_m close to 0, which
385 underestimates GR_{true} .

386 **Appendix A**

387 To evaluate the contribution of self-coagulation of the mode ($GR_{m, self}$) and cluster coagulation ($GR_{m, cluster}$) to
 388 measured growth rate based on mode diameter ($GR_{m, mode}$), we used the following first order numerical approximation
 389 method:

- 390 1. Find particle size distribution $\tilde{n} = \tilde{n}(k, \tau)$ at a given time τ . k is the number of monomers in a particle and \tilde{n}_k
 391 is the concentration of particles that contains k molecules. Since the simulation code only reports discrete particle
 392 concentration for each bin, an interpolation is performed using Matlab function *griddedInterpolant.m*.
- 393 2. Find the value $k = k_{max}$ at which $3 \log(10) k \tilde{n}(k, \tau)$ is locally maximized. A prefactor $3 \log(10) k$ is
 394 multiplied to $\tilde{n}(k, \tau)$ to convert the particle size distribution to $d\tilde{N}/d\log_{10} \tilde{d}_p$. The mode diameter is then given
 395 by $\tilde{d}_{p, mode}(\tau) = \left(\frac{6k_{max}}{\pi}\right)^{1/3}$
- 396 3. Use the following integration equations to obtain number distribution of the mode at time $\tau + \Delta\tau$ assuming only
 397 one process causes the distribution to shift.

398 For self-coagulation:

$$399 \tilde{n}_{self}(k, \tau + \Delta\tau) = \tilde{n}(k) + 0.5 * \Delta\tau * \int_L^k c(x, k - x) \tilde{n}(x, \tau) \tilde{n}(k - x, \tau) dx - \int_L^H c(x, k) \tilde{n}(k, \tau) \tilde{n}(x, \tau) dx. \quad (A1)$$

400 For coagulation with clusters:

$$401 \tilde{n}_{cluster}(k, \tau + \Delta\tau) = \tilde{n}(k, \tau) + 0.5 \cdot \Delta\tau \cdot \int_{L_c}^{H_c} c(x, k - x) \tilde{n}(x, \tau) \tilde{n}(k - x, \tau) H(H_c - k + x) dx + \Delta\tau \cdot \\ 402 \int_{L_c}^{H_c} c(x, k - x) \tilde{n}(x, \tau) \tilde{n}(k - x, \tau) H(k - x - H_c) dx - \Delta\tau \cdot \int_{L_c}^{H_c} c(x, k) \tilde{n}(x, \tau) \tilde{n}(k, \tau) dx. \quad (A2)$$

403 In the above equations, L and H are the lower and upper boundary of the mode, L_c and H_c are the lower and
 404 upper boundary of clusters, $c(i, j)$ is the collision frequency function, $H(x)$ is the Heaviside step function. $\Delta\tau$ is
 405 typically set between 0.1 to 1.

- 406 4. Find the k values at which $3 \log(10) k \tilde{n}_{self}(k, \tau + \Delta\tau)$ and $3 \log(10) k \tilde{n}_{cluster}(k, \tau + \Delta\tau)$ are locally
 407 maximized. The corresponding diameters are $\tilde{d}_{p, self}(\tau + \Delta\tau)$ and $\tilde{d}_{p, cluster}(\tau + \Delta\tau)$.
- 408 5. The growth rate due to self-coagulation and coagulation with clusters are then given by

$$409 GR_{m, self} = \frac{\tilde{d}_{p, self}(\tau + \Delta\tau) - \tilde{d}_{p, mode}(\tau)}{\Delta\tau}; GR_{m, cluster} = \frac{\tilde{d}_{p, cluster}(\tau + \Delta\tau) - \tilde{d}_{p, mode}(\tau)}{\Delta\tau}. \quad (A3)$$

410 **Appendix B**

411

412 To facilitate comparison between dimensionless simulation results and experimental results, or previous dimensional
413 simulation results, we convert selected dimensionless simulation results to dimensional quantities using Eq. (6).
414 Specifically, we assume the monomer production rate is $R = 1 \times 10^6 \text{ cm}^{-3} \text{ s}^{-1}$ and the monomer has a volume of
415 $1.62 \times 10^{-22} \text{ cm}^3$ and a density of 1.47 g cm^{-3} . The collision frequency function for monomers, $\beta_{11 fm}$, is
416 $4.27 \times 10^{-10} \text{ cm}^3 \text{ s}^{-1}$, calculated at atmospheric pressure and 300 K. We consider two nucleation scenarios. The first
417 is collision-controlled nucleation in the presence of pre-existing particles, with \sqrt{L} set to 0.2. The second scenario is
418 nucleation with evaporation in the presence of pre-existing particles. The evaporation constant in this case is $E =$
419 1×10^{-3} and \sqrt{L} is 0.2. Both these cases are discussed in Sect. 3.3. The converted dimensional results are shown in
420 Fig. B1, with relevant dimensional quantities displayed in the figure.

421 Acknowledgements

422 This research was supported by the US Department of Energy's Atmospheric System Research, an Office of Science,
423 Office of Biological and Environmental Research program, under grant number DE-SC0011780.

424 Nomenclature

425 Collision-controlled nucleation: a limiting case for nucleation where all collisions between condensing (nucleating)
426 vapor occur at the rate predicted by kinetic theory and particles stick with 100% efficiency. Vapor does not
427 subsequently evaporate from particle surfaces, nor are particles scavenged by pre-existing particles or the chamber
428 wall

429 $\tilde{d}_{p,min}$: particle size corresponding to the local minimum in a $d\tilde{N}/d\log_{10}\tilde{d}_p$ representation of particle size distribution

430 $\tilde{d}_{p,mode}$: particle size corresponding to the local maximum in a $d\tilde{N}/d\log_{10}\tilde{d}_p$ representation of particle size
431 distribution

432 $\tilde{d}_{p,sr50}$: particle size of a measurement bin where particle concentration reaches 50% of its maximum value

433 $\tilde{d}_{p,sr100}$: particle size of a measurement bin where particle concentration reaches maximum value

434 $\tilde{d}_{p,tot50}$: particle size above which total particle concentration reaches 50% of its maximum value

435 $GR_{m,mode}$: measured dimensionless growth rate based on $\tilde{d}_{p,mode}$

436 $GR_{m,sr50}$: measured dimensionless growth rate based on $\tilde{d}_{p,sr50}$

437 $GR_{m,sr100}$: measured dimensionless growth rate based on $\tilde{d}_{p,sr100}$

438 $GR_{m,tot50}$: measured dimensionless growth rate based on $\tilde{d}_{p,tot50}$

439 GR_{true} : true dimensionless particle growth rate attributed to the net flux of condensing vapors onto particle surface
440 (i.e., the condensation rate minus the evaporation rate)

441 $GR_{m,clsuter}$: measured dimensionless particle growth rate attributed to coagulation with clusters
442 $GR_{m,self}$: measured dimensionless growth rate attributed to self-coagulation of particles in the nucleation mode
443 E, Ω : dimensionless parameters characterizing evaporation rates of particles, derived from the liquid droplet model.
444 E can be regarded as a dimensionless form of saturation vapor pressure of the condensing molecules and Ω a
445 dimensionless form of surface tension. Ω assumes a constant value of 16 in this work.
446 \sqrt{L} : dimensionless parameter characterizing fractional loss rate of monomer or nucleated particles to pre-existing
447 particles
448 \tilde{N}_k : dimensionless concentration of particles containing k monomers (i.e., k molecules of condensed vapor)

449 **References**

450 Almeida, J., Schobesberger, S., Kürten, A., Ortega, I. K., Kupiainen-Määttä, O., Praplan, A. P., Adamov, A.,
451 Amorim, A., Bianchi, F., Breitenlechner, M., David, A., Dommen, J., Donahue, N. M., Downard, A., Dunne,
452 E., Duplissy, J., Ehrhart, S., Flagan, R. C., Franchin, A., Guida, R., Hakala, J., Hansel, A., Heinritzi, M.,
453 Henschel, H., Jokinen, T., Junninen, H., Kajos, M., Kangasluoma, J., Keskinen, H., Kupc, A., Kurtén, T.,
454 Kvashin, A. N., Laaksonen, A., Lehtipalo, K., Leiminger, M., Leppä, J., Loukonen, V., Makhmutov, V.,
455 Mathot, S., McGrath, M. J., Nieminen, T., Olenius, T., Onnela, A., Petäjä, T., Riccobono, F., Riipinen, I.,
456 Rissanen, M., Rondo, L., Ruuskanen, T., Santos, F. D., Sarnela, N., Schallhart, S., Schnitzhofer, R., Seinfeld,
457 J. H., Simon, M., Sipilä, M., Stozhkov, Y., Stratmann, F., Tomé, A., Tröstl, J., Tsagkogeorgas, G.,
458 Vaattovaara, P., Viisanen, Y., Virtanen, A., Vrtala, A., Wagner, P. E., Weingartner, E., Wex, H., Williamson,
459 C., Wimmer, D., Ye, P., Yli-Juuti, T., Carslaw, K. S., Kulmala, M., Curtius, J., Baltensperger, U., Worsnop, D.
460 R., Vehkamäki, H., and Kirkby, J.: Molecular understanding of sulphuric acid–amine particle nucleation in
461 the atmosphere, *Nature*, 502, 359, 10.1038/nature12663
462 <https://www.nature.com/articles/nature12663-supplementary-information>, 2013.
463 Barsanti, K. C., McMurry, P. H., and Smith, J. N.: The potential contribution of organic salts to new
464 particle growth, *Atmos. Chem. Phys.*, 9, 2949–2957, 10.5194/acp-9-2949-2009, 2009.
465 Chan, T. W., and Mozurkewich, M.: Measurement of the coagulation rate constant for sulfuric acid
466 particles as a function of particle size using tandem differential mobility analysis, *Journal of Aerosol
467 Science*, 32, 321–339, [https://doi.org/10.1016/S0021-8502\(00\)00081-1](https://doi.org/10.1016/S0021-8502(00)00081-1), 2001.
468 Friedlander, S. K.: *Smoke, dust, and haze : fundamentals of aerosol dynamics*, 2nd ed.. ed., New York :
469 Oxford University Press, New York, 2000.
470 Fuchs, N. A., and Sutugin, A. G.: HIGH-DISPersed AEROSOLS A2 - HIDY, G.M, in: *Topics in Current
471 Aerosol Research*, edited by: Brock, J. R., Pergamon, 1, 1971.
472 Gelbard, F., and Seinfeld, J. H.: The general dynamic equation for aerosols. Theory and application to
473 aerosol formation and growth, *Journal of Colloid and Interface Science*, 68, 363–382,
474 [https://doi.org/10.1016/0021-9797\(79\)90289-3](https://doi.org/10.1016/0021-9797(79)90289-3), 1979.
475 Gelbard, F., and Seinfeld, J. H.: Simulation of multicomponent aerosol dynamics, *Journal of Colloid and
476 Interface Science*, 78, 485–501, [https://doi.org/10.1016/0021-9797\(80\)90587-1](https://doi.org/10.1016/0021-9797(80)90587-1), 1980.
477 Heisler, S. L., and Friedlander, S. K.: Gas-to-particle conversion in photochemical smog: Aerosol growth
478 laws and mechanisms for organics, *Atmospheric Environment* (1967), 11, 157–168,
479 [https://doi.org/10.1016/0004-6981\(77\)90220-7](https://doi.org/10.1016/0004-6981(77)90220-7), 1977.

480 Hodshire, A. L., Lawler, M. J., Zhao, J., Ortega, J., Jen, C., Yli-Juuti, T., Brewer, J. F., Kodros, J. K., Barsanti,
481 K. C., Hanson, D. R., McMurry, P. H., Smith, J. N., and Pierce, J. R.: Multiple new-particle growth
482 pathways observed at the US DOE Southern Great Plains field site, *Atmos. Chem. Phys.*, 16, 9321-9348,
483 10.5194/acp-16-9321-2016, 2016.
484 Kerminen, V. M., and Kulmala, M.: Analytical formulae connecting the "real" and the "apparent"
485 nucleation rate and the nuclei number concentration for atmospheric nucleation events, *Journal of*
486 *Aerosol Science*, 33, 609-622, 2002.
487 Kontkanen, J., Olenius, T., Lehtipalo, K., Vehkamäki, H., Kulmala, M., and Lehtinen, K. E. J.: Growth of
488 atmospheric clusters involving cluster–cluster collisions: comparison of different growth rate methods,
489 *Atmos. Chem. Phys.*, 16, 5545-5560, 10.5194/acp-16-5545-2016, 2016.
490 Kuang, C., Riipinen, I., Yli-Juuti, T., Kulmala, M., McCormick, A. V., and McMurry, P. H.: An improved
491 criterion for new particle formation in diverse atmospheric environments, *Atmospheric Chemistry and*
492 *Physics*, 10, 1-12, 10.5194/acp-10-1-2010, 2010.
493 Kuang, C., Chen, M., Zhao, J., Smith, J., McMurry, P. H., and Wang, J.: Size and time-resolved growth rate
494 measurements of 1 to 5 nm freshly formed atmospheric nuclei, *Atmos. Chem. Phys.*, 12, 3573-3589,
495 10.5194/acp-12-3573-2012, 2012.
496 Kulmala, M., Petäjä, T., Nieminen, T., Sipilä, M., Manninen, H. E., Lehtipalo, K., Dal Maso, M., Aalto, P. P.,
497 Junninen, H., Paasonen, P., Riipinen, I., Lehtinen, K. E. J., Laaksonen, A., and Kerminen, V.-M.:
498 Measurement of the nucleation of atmospheric aerosol particles, *Nature Protocols*, 7, 1651,
499 10.1038/nprot.2012.091
500 <https://www.nature.com/articles/nprot.2012.091-supplementary-information>, 2012.
501 Kürten, A., Li, C., Bianchi, F., Curtius, J., Dias, A., Donahue, N. M., Duplissy, J., Flagan, R. C., Hakala, J.,
502 Jokinen, T., Kirkby, J., Kulmala, M., Laaksonen, A., Lehtipalo, K., Makhmutov, V., Onnela, A., Rissanen, M.
503 P., Simon, M., Sipilä, M., Stozhkov, Y., Tröstl, J., Ye, P., and McMurry, P. H.: New particle formation in the
504 sulfuric acid–dimethylamine–water system: reevaluation of CLOUD chamber measurements and
505 comparison to an aerosol nucleation and growth model, *Atmos. Chem. Phys.*, 18, 845-863, 10.5194/acp-
506 18-845-2018, 2018.
507 Lehtinen, K. E. J., and Kulmala, M.: A model for particle formation and growth in the atmosphere with
508 molecular resolution in size, *Atmos. Chem. Phys.*, 3, 251-257, 10.5194/acp-3-251-2003, 2003.
509 Lehtinen, K. E. J., Rannik, U., Petaja, T., Kulmala, M., and Hari, P.: Nucleation rate and vapor
510 concentration estimations using a least squares aerosol dynamics method - art. no. D21209, *Journal of*
511 *Geophysical Research-Atmospheres*, 109, 21209, 2004.
512 Lehtipalo, K., Rondo, L., Kontkanen, J., Schobesberger, S., Jokinen, T., Sarnela, N., Kürten, A., Ehrhart, S.,
513 Franchin, A., Nieminen, T., Riccobono, F., Sipilä, M., Yli-Juuti, T., Duplissy, J., Adamov, A., Ahlm, L.,
514 Almeida, J., Amorim, A., Bianchi, F., Breitenlechner, M., Dommen, J., Downard, A. J., Dunne, E. M.,
515 Flagan, R. C., Guida, R., Hakala, J., Hansel, A., Jud, W., Kangasluoma, J., Kerminen, V.-M., Keskinen, H.,
516 Kim, J., Kirkby, J., Kupc, A., Kupiainen-Määttä, O., Laaksonen, A., Lawler, M. J., Leiminger, M., Mathot, S.,
517 Olenius, T., Ortega, I. K., Onnela, A., Petäjä, u., Praplan, A., Rissanen, M. P., Ruuskanen, T., Santos, F. D.,
518 Schallhart, S., Schnitzhofer, R., Simon, M., Smith, J. N., Tröstl, J., Tsagkogeorgas, G., Tome, A. n.,
519 Vaattovaara, P., Hanna Vehkama ki1, Vrtala, A. E., Wagner, P. E., Williamson, C., Wimmer, D., Winkler,
520 P. M., Virtanen, A., Donahue, N. M., Carslaw, K. S., Baltensperger, U., Riipinen, I., Curtius, J., Worsnop, D.
521 R., and Kulmala, M.: The effect of acid-base clustering and ions on the growth of atmospheric nano-
522 particles, *Nature Communications*, 7, 11594, 2016.
523 Lehtipalo , K., Leppa , J , Kontkanen , J , Kangasluoma , J , Franchin , A , Wimnner , D , Schobesberger , S ,
524 Junninen , H , Petaja , T , Sipila , M , Mikkila , J , Vanhanen , J , Worsnop , D R & Kulmala: Methods for
525 determining particle size distribution and growth rates between 1 and 3 nm using the Particle Size
526 Magnifier, *Boreal Environment Research*, 19, 215-236, 2014.

527 McMurry, P. H., and Friedlander, S. K.: New particle formation in the presence of an aerosol, *Atmos.*
528 *Environ.*, 13, 1635-1651, 1979.

529 McMurry, P. H.: Photochemical aerosol formation from SO₂: A theoretical analysis of smog chamber
530 data, *Journal of Colloid and Interface Science*, 78, 513-527, [https://doi.org/10.1016/0021-9797\(80\)90589-5](https://doi.org/10.1016/0021-9797(80)90589-5), 1980.

532 McMurry, P. H., and Wilson, J. C.: Growth laws for the formation of secondary ambient aerosols:
533 Implications for chemical conversion mechanisms, *Atmospheric Environment* (1967), 16, 121-134,
534 [https://doi.org/10.1016/0004-6981\(82\)90319-5](https://doi.org/10.1016/0004-6981(82)90319-5), 1982.

535 McMurry, P. H., and Li, C.: The dynamic behavior of nucleating aerosols in constant reaction rate
536 systems: Dimensional analysis and generic numerical solutions, *Aerosol Science and Technology*, 51,
537 1057-1070, 10.1080/02786826.2017.1331292, 2017.

538 Olenius, T., Riipinen, I., Lehtipalo, K., and Vehkamäki, H.: Growth rates of atmospheric molecular clusters
539 based on appearance times and collision–evaporation fluxes: Growth by monomers, *Journal of Aerosol*
540 *Science*, 78, 55-70, <https://doi.org/10.1016/j.jaerosci.2014.08.008>, 2014.

541 Pichelstorfer, L., Stolzenburg, D., Ortega, J., Karl, T., Kokkola, H., Laakso, A., Lehtinen, K. E. J., Smith, J. N.,
542 McMurry, P. H., and Winkler, P. M.: Resolving nanoparticle growth mechanisms from size- and time-
543 dependent growth rate analysis, *Atmos. Chem. Phys. Discuss.*, 2017, 1-24, 10.5194/acp-2017-658, 2017.

544 Rao, N. P., and McMurry, P. H.: Nucleation and Growth of Aerosol in Chemically Reacting Systems: A
545 Theoretical Study of the Near-Collision-Controlled Regime, *Aerosol Science and Technology*, 11, 120-
546 132, 10.1080/02786828908959305, 1989.

547 Riccobono, F.: Contribution of sulfuric acid and oxidized organic compounds to particle formation and
548 growth, *Atmos. Chem. Phys.*, 12, 9427-9439, 2012.

549 Riccobono, F.: Oxidation products of biogenic emissions contribute to nucleation of atmospheric
550 particles, *Science*, 344, 717-721, 2014.

551 Riipinen, I., Yli-Juuti, T., Pierce, J. R., Petäjä, T., Worsnop, D. R., Kulmala, M., and Donahue, N. M.: The
552 contribution of organics to atmospheric nanoparticle growth, *Nature Geoscience*, 5, 453,
553 10.1038/ngeo1499, 2012.

554 Smith, J., Dunn, M., VanReken, T., Iida, K., Stolzenburg, M., McMurry, P., and Huey, L.: Chemical
555 composition of atmospheric nanoparticles formed from nucleation in Tecamac, Mexico: Evidence for an
556 important role for organic species in nanoparticle growth, *Geophysical Research Letters*, 35, 2008.

557 Smith, J. N., Barsanti, K. C., Friedli, H. R., Ehn, M., Kulmala, M., Collins, D. R., Scheckman, J. H., Williams,
558 B. J., and McMurry, P. H.: Observations of aminium salts in atmospheric nanoparticles and possible
559 climatic implications, *Proceedings of the National Academy of Sciences*, 107, 6634-6639, 2010.

560 Stolzenburg, M. R., McMurry, P. H., Sakurai, H., Smith, J. N., Mauldin, R. L., Eisele, F. L., and Clement, C.
561 F.: Growth rates of freshly nucleated atmospheric particles in Atlanta, *Journal of Geophysical Research: Atmospheres*, 110, n/a-n/a, 10.1029/2005JD005935, 2005.

562 Tröstl, J., Chuang, W. K., Gordon, H., Heinritzi, M., Yan, C., Molteni, U., Ahlm, L., Frege, C., Bianchi, F.,
563 Wagner, R., Simon, M., Lehtipalo, K., Williamson, C., Craven, J. S., Duplissy, J., Adamov, A., Almeida, J.,
564 Bernhammer, A.-K., Breitenlechner, M., Brilke, S., Dias, A., Ehrhart, S., Flagan, R. C., Franchin, A., Fuchs,
565 C., Guida, R., Gysel, M., Hansel, A., Hoyle, C. R., Jokinen, T., Junninen, H., Kangasluoma, J., Keskinen, H.,
566 Kim, J., Krapf, M., Kürten, A., Laaksonen, A., Lawler, M., Leiminger, M., Mathot, S., Möhler, O., Nieminen,
567 T., Onnela, A., Petäjä, T., Piel, F. M., Miettinen, P., Rissanen, M. P., Rondo, L., Sarnela, N., Schobesberger,
568 S., Sengupta, K., Sipilä, M., Smith, J. N., Steiner, G., Tomè, A., Virtanen, A., Wagner, A. C., Weingartner,
569 E., Wimmer, D., Winkler, P. M., Ye, P., Carslaw, K. S., Curtius, J., Dommen, J., Kirkby, J., Kulmala, M.,
570 Riipinen, I., Worsnop, D. R., Donahue, N. M., and Baltensperger, U.: The role of low-volatility organic
571 compounds in initial particle growth in the atmosphere, *Nature*, 533, 527, 10.1038/nature18271, 2016.

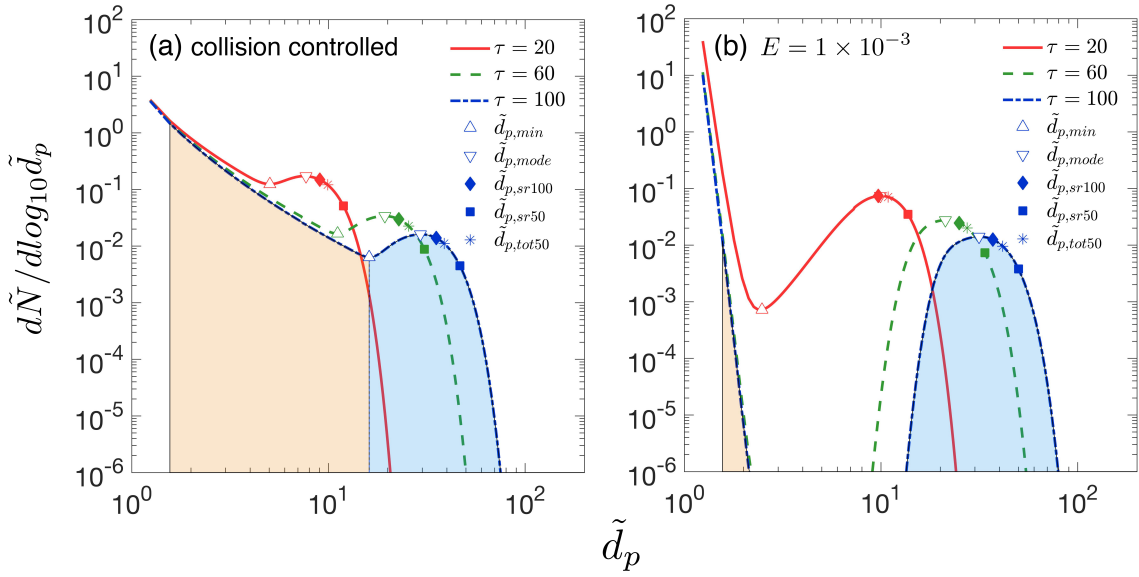
573 Verheggen, B., and Mozurkewich, M.: An inverse modeling procedure to determine particle growth and
574 nucleation rates from measured aerosol size distributions, *Atmospheric Chemistry and Physics*, 6, 2927-
575 2942, 2006.

576 Wang, J., McGraw, R. L., and Kuang, C.: Growth of atmospheric nano-particles by heterogeneous
577 nucleation of organic vapor, *Atmos. Chem. Phys.*, 13, 6523-6531, 10.5194/acp-13-6523-2013, 2013.

578 Weber, R. J., Marti, J. J., McMurry, P. H., Eisele, F. L., Tanner, D. J., and Jefferson, A.: Measurements of
579 new particle formation and ultrafine particle growth rates at a clean continental site, *Journal of
580 Geophysical Research: Atmospheres*, 102, 4375-4385, 10.1029/96JD03656, 1997.

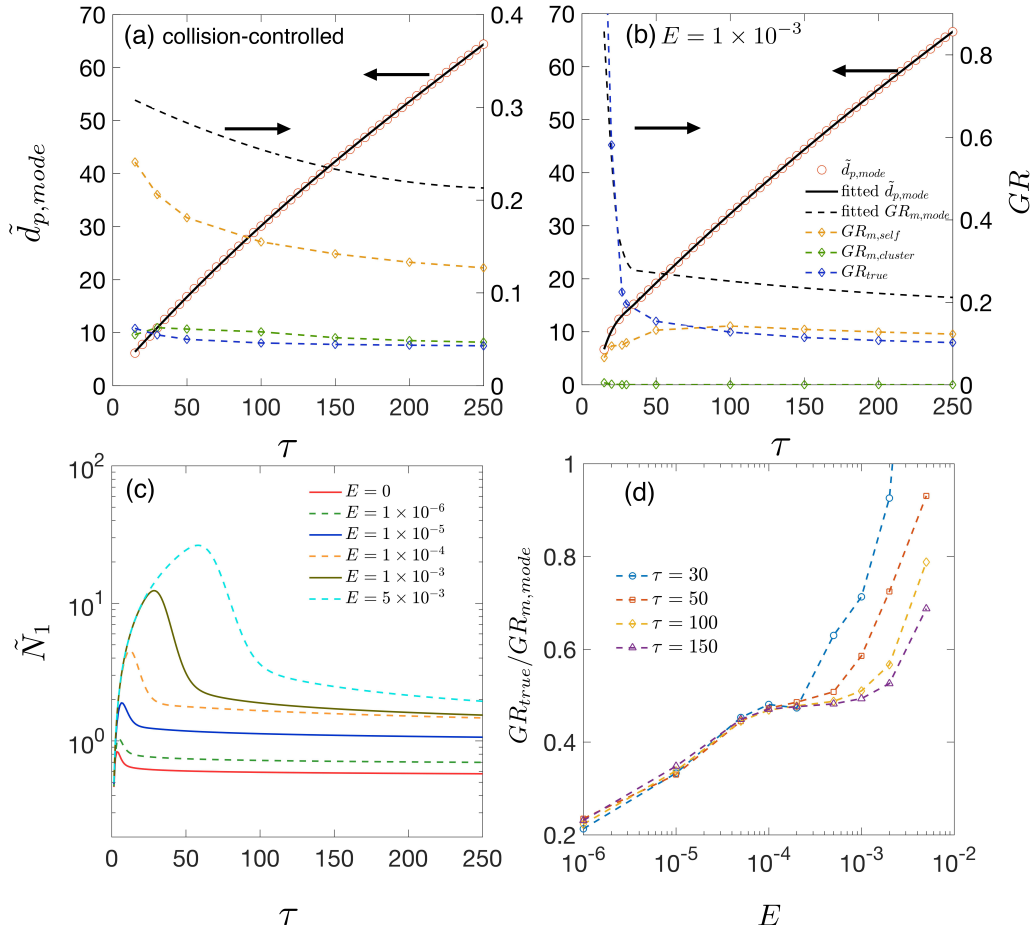
581 Yli-Juuti, T.: Growth rates of nucleation mode particles in Hyytiälä during 2003–2009: variation with
582 particle size, season, data analysis method and ambient conditions, *Atmos. Chem. Phys.*, 11, 12865-
583 12886, 2011.

584

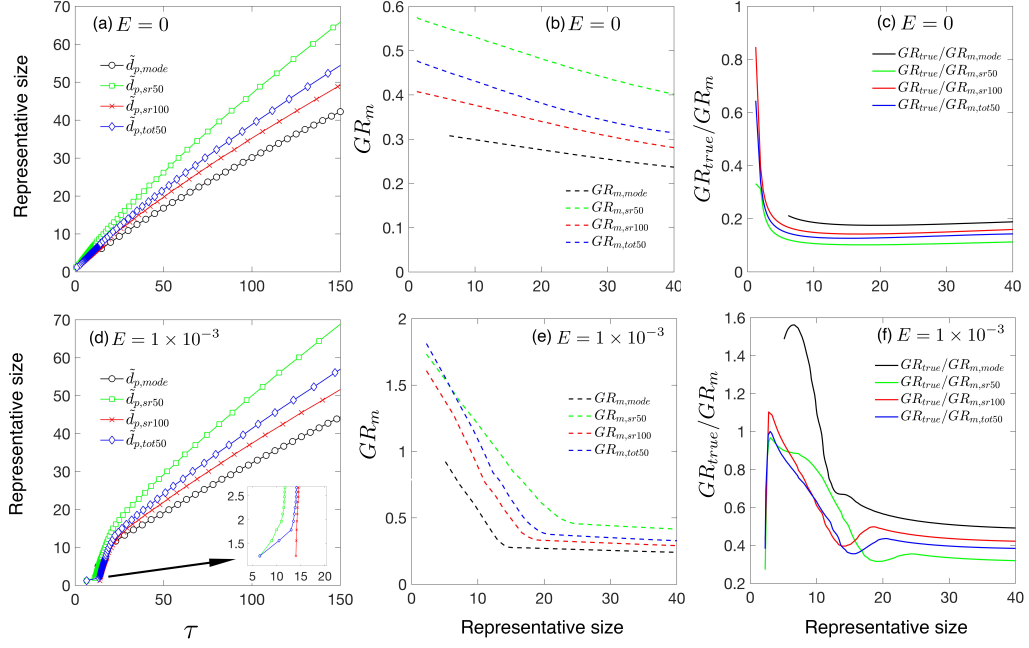


585
586 **Figure 1.** Particle size distributions at dimensionless times $\tau = 20, 60, 100$ **(a)** for collision-controlled nucleation
587 ($E=0$) and **(b)** when evaporation is included with $E = 1 \times 10^{-3}$. Division of the distribution into monomer, cluster
588 and nucleation mode is displayed for $\tau = 100$, with beige and light blue indicating the range of clusters and nucleation
589 mode. Clusters and nucleation mode are separated by $\tilde{d}_{p,min}$, where $d\tilde{N}/d\log_{10}\tilde{d}_p$ is at a local minimum.
590 Characteristic sizes $\tilde{d}_{p,mode}$, $\tilde{d}_{p,sr100}$, $\tilde{d}_{p,sr50}$ and $\tilde{d}_{p,tot50}$ are marked for each time. The relationship between
591 symbols and characteristic sizes is shown only for $\tau=100$.

592



595 **Figure 2. (a)** $\tilde{d}_{p,mode}$ and various growth rates as functions of time for collision-controlled nucleation. Dashed black
 596 lines show the value of $GR_{m,mode}$. Yellow, green and blue dashed lines represent $GR_{m,self}$, $GR_{m,cluster}$ and GR_{true}
 597 respectively. **(b)** The same quantities as are shown in (a) but with the evaporation constant set to $E = 1 \times 10^{-3}$. For
 598 both Fig. 2a and 2b, the left axis shows value for the solid lines and the right axis shows values for the dashed lines.
 599 **(c)** Monomer concentration as functions of time for different values of E . **(d)** $GR_{true}/GR_{m,mode}$ for different values of E
 600 at $\tau = 30, 50, 100, 150$.



602

603 **Figure 3.** (a) $\tilde{d}_{p,mode}$, $\tilde{d}_{p,sr100}$, $\tilde{d}_{p,tot50}$, $\tilde{d}_{p,bin50}$ as functions of time. (b) Measured growth rates $GR_{m,mode}$, $GR_{m,sr50}$,
604 $GR_{m,sr100}$, $GR_{m,tot50}$ as functions of representative sizes. (c) Ratio of true growth rate to measured growth rate,
605 GR_{true}/GR_m . Figures 3a-3c are for collision-controlled nucleation with $E=0$. Figures 3d-3f show the same quantities
606 as are shown in Fig. 3a-3c but with $E = 1 \times 10^{-3}$.

607

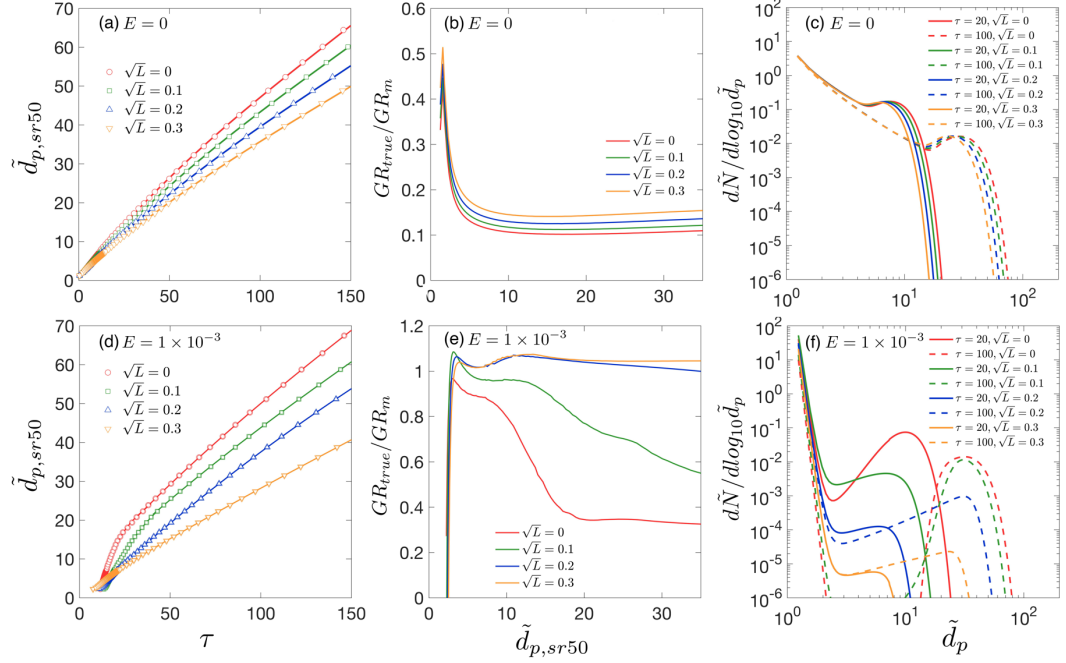


Figure 4. Effect of preexisting particles on particle growth rate. **(a)** $\tilde{d}_{p,sr50}$ as a function of time. **(b)** Ratio of true growth rate to measured growth rate, $GR_{true}/GR_{m,sr50}$. **(c)** Particle size distributions at $\tau = 20$ and $\tau = 100$. Figures 4a-4c are for collision-controlled nucleation with $E = 0$ and $\sqrt{L} = 0, 0.1, 0.2, 0.3$. Figures 4c-4d show the same quantities as are shown in Fig. 4a-4c but with $E = 1 \times 10^{-3}$.

608

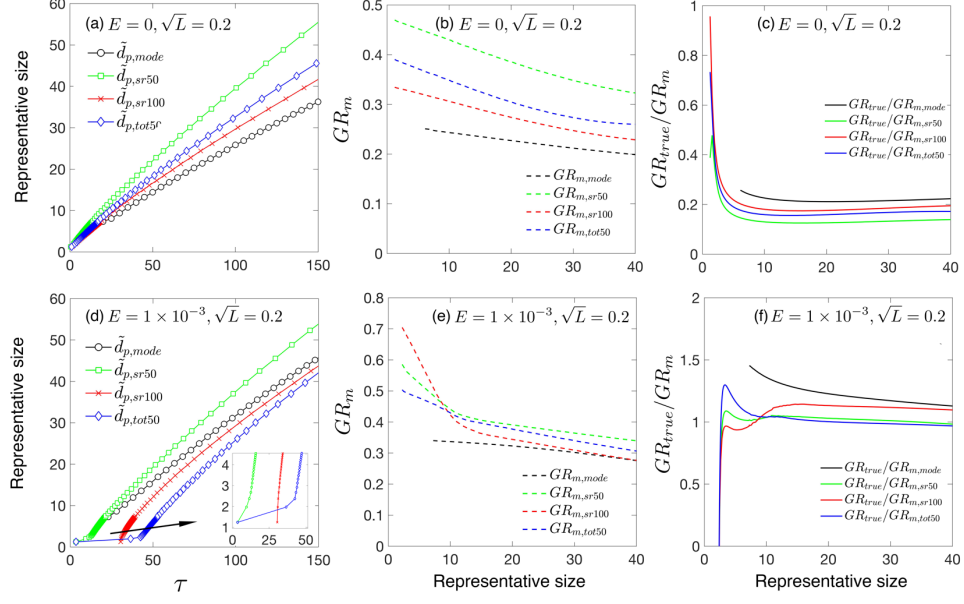
609

610

611

612

613



614

615 **Figure 5.** (a) $\tilde{d}_{p,mode}$, $\tilde{d}_{p,sr100}$, $\tilde{d}_{p,tot50}$, $\tilde{d}_{p,bin50}$ as functions of time. (b) Measured growth rate $GR_{m,mode}$, $GR_{m,sr50}$,
616 $GR_{m,sr100}$, $GR_{m,tot50}$ as functions of representative sizes. (c) Ratio of true growth rate to measured growth rate,
617 GR_{true}/GR_m . Figures 5a-5c are for collision-controlled nucleation with $E = 0$ and $\sqrt{L} = 0.2$. Figures 5d-5f show the
618 same quantities as are shown in Fig. 5a-5c but with $E = 1 \times 10^{-3}$.

619

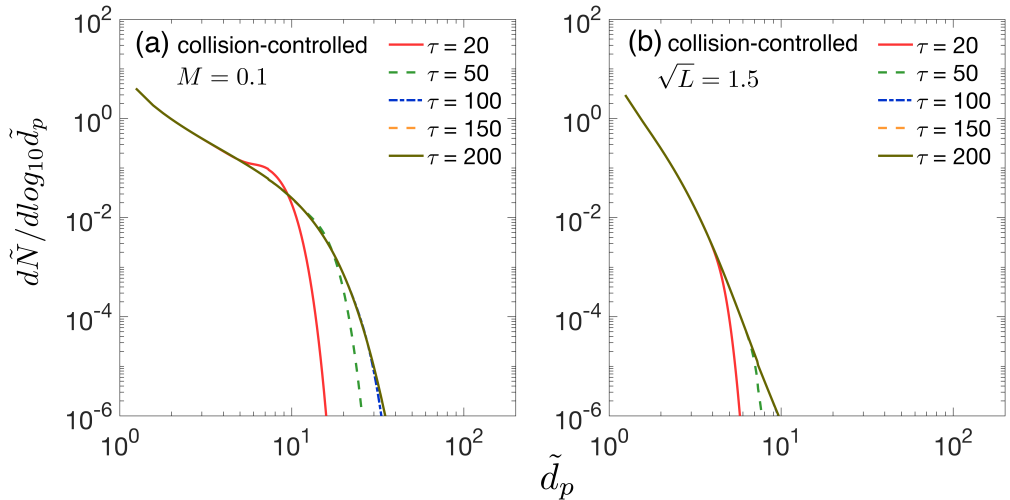


Figure 6. Particle size distribution at different dimensionless times for collision-controlled nucleation with **(a)** $M=0.1$ and **(b)** $\sqrt{L} = 1.5$. In both cases, sink processes not indicated in the figure were set to zero in the simulations. Particle size distributions at certain times are not visible in the figure since they overlap with the particle size distribution at a later time.

620

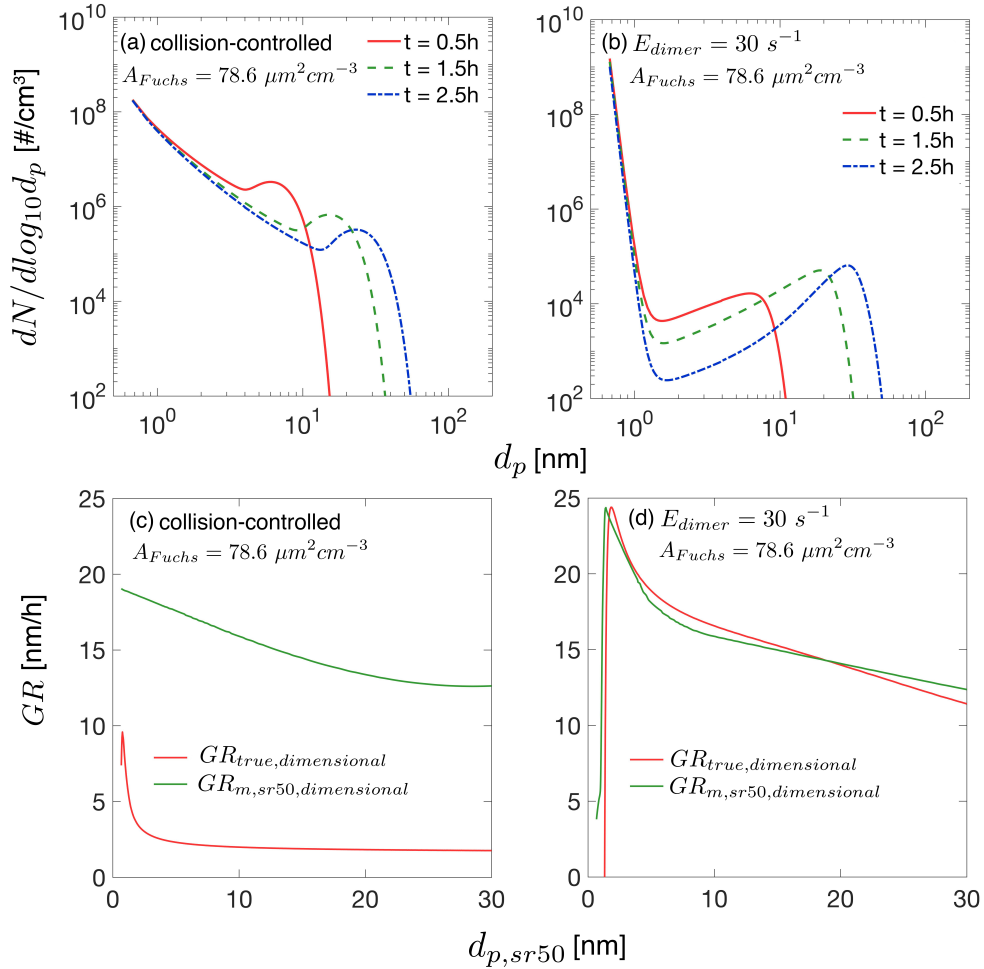
621

622

623

624

625



628 **Figure B1.** Dimensional particle size distribution and growth rates. The quantities shown in this figure are converted
 629 from the dimensionless solution using Eqn. (6). The dimensional quantities involved in the conversions are $R =$
 630 $1 \times 10^6 \text{ cm}^{-3} \text{ s}^{-1}$, $\beta_{11 fm} = 4.27 \times 10^{-10} \text{ cm}^3 \text{ s}^{-1}$ and $v_1 = 1.62 \times 10^{-22} \text{ cm}^3$. The Fuchs surface area is 78.6
 631 $\mu\text{m}^2 \text{ cm}^{-3}$, corresponding to $\sqrt{L} = 0.2$. **(a)** Particle size distribution for collision controlled nucleation at $t = 0.5\text{h}$, 1.5h
 632 and 2.5h. **(b)** Particle size distribution for nucleation with evaporation at $t = 0.5\text{h}$, 1.5h and 2.5h. Monomer evaporation
 633 rate from dimer is 30 s^{-1} , corresponding to a dimensionless evaporation constant $E = 1 \times 10^{-3}$. **(c)** The dimensional
 634 particle growth rates for collision-controlled nucleation as is shown in Fig. B1a. **(d)** The dimensional particle growth
 635 rates for nucleation with evaporation as is shown in Fig. B1b.